INSTITUTO POLITÉCNICO DE LISBOA

ESCOLA SUPERIOR DE TECNOLOGIA DA SAÚDE DE LISBOA

EVALUATION OF IMRT AND VMAT TECHNIQUES WITH AND WITHOUT FLATTENING FILTER USING PARETO OPTIMAL FRONTS

EUNICE MAGALHÃES

PROF. NUNO TEIXEIRA, PhD (SUPERVISOR)
PROF. DIETMAR GEORG, PhD (SUPERVISOR)
PROF. MARGARIDA EIRAS, MSc (SUPERVISOR)
DR. GABRIELE KRAGL, PhD (ADVISOR)

Master in Radiation in Health Technology

Lisbon, 2012

INSTITUTO POLITÉCNICO DE LISBOA

ESCOLA SUPERIOR DE TECNOLOGIA DA SAÚDE DE LISBOA

EVALUATION OF IMRT AND VMAT TECHNIQUES WITH AND WITHOUT FLATTENING FILTER USING PARETO OPTIMAL FRONTS

EUNICE MAGALHÃES

PROF. NUNO TEIXEIRA, PhD (SUPERVISOR)
PROF. DIETMAR GEORG, PhD (SUPERVISOR)
PROF. MARGARIDA EIRAS, MSc (SUPERVISOR)
DR. GABRIELE KRAGL, PhD (ADVISOR)

REFEREE

Prof. Dr. Elizabeth C. Moser, Physician and Researcher at Champalimaud Foundation, Lisbon

Master in Radiation in Health Technology

Lisbon, 2012

Agradecimentos

Aos meus orientadores Prof. Margarida Eiras e Prof. Nuno Teixeira, por todos os conhecimentos transmitidos, pela sua ajuda, pela sua orientação e por me transmitirem a confiança e a motivação para este projecto.

Aos meus orientadores do Hospital Allgemeines Krankenhaus in Vienna, Austria, Prof. Dietmar Georg e Gabriele Kragl, por me terem proporcionado acesso a este projecto e por me terem integrado na sua equipa de investigadores. Ao meu colega Lechner Wolfgang, por ter iniciado este projecto, por tão bem me ter integrado, pela sua ajuda e por estar sempre aberto a questões. Desejo-lhe muita sorte e um futuro com muito sucesso.

À Sociedade Avanço, nomeadamente ao Eng. Diogo Marcos por sempre ter alimentado o meu "bichinho" da investigação, pela força e entusiasmo e, por me ter proporcionado a oportunidade de desenvolver este projecto na MUW, Áustria. O meu mais sincero Obrigado!

Aos meus amigos Joana e Samuel, por todos os incentivos, pelo apoio e pela distracção proporcionada, por vezes tão necessária. Aos amigos com quem tive o privilégio de partilhar esta etapa.

À Isabel e ao Carlos, à Susana e ao Bruno, à Ilda e à Dona Guilhermina por terem partilhado comigo momentos difíceis, durante o decurso da minha tese e me terem ajudado a levantar o ânimo.

À minha família, à minha Mãe e aos meus irmãos, Cláudia e Paulo a quem tanto privei da minha companhia e de quem sempre recebi o apoio necessário. Aos meus sobrinhos Diogo e Martim por me alegrarem apenas com o seu sorriso.

Ao meu namorado, Ricardo, por estar sempre ao meu lado, pelas noites mal dormidas, por aturar os meus desabafos, por ser parte activa na minha vida, por ser o meu pilar de apoio. Sem Ele este trabalho não se teria concretizado.

Ao meu Pai, porque mesmo estando longe está sempre perto.

Resumo

Introdução: O interesse demonstrado em aceleradores lineares sem *flattening filter* justifica o estudo da qualidade das planimetrias de Radioterapia com Intensidade Modulada (IMRT) e Arco-terapia Volumétrica Modulada (VMAT) efectuadas com e sem *flattening filter* (FF).

Materiais e métodos: Foram seleccionados três casos de cancro de próstata em estadio inicial. Efectuaram-se planimetrias de IMRT e VMAT com e sem FF, baseado no formalismo de *Pareto optimal fronts*. Sistematicamente variando a função de custo de um órgão de risco, diferentes distribuições de dose foram calculadas.

Para comparar as diferentes técnicas, *Pareto optimal fronts* foram analisadas. As *Pareto optimal fronts* são determinadas através da representação gráfica de determinados valores da distribuição de dose para o PTV e para o órgão de risco. Comparando os resultados para cada técnica ajudará a decidir qual a melhor técnica para aquele paciente.

Resultados: Foram efectuadas planimetrias para IMRT e VMAT com e sem *flattening filter* com qualidade similar. No caso 1 e 2, as *Pareto optimal fronts* diferem significativamente para IMRT e VMAT, apresentando melhores resultados para IMRT sem FF. No caso do terceiro paciente as *Pareto optimal fronts* encontram-se sobrepostas. O tempo de administração do tratamento para IMRT sem FF foi reduzido em 24% e diminuiu de uma forma mais acentuada para as técnicas de VMAT. Registou-se um aumento de 9-15% no número de unidades monitor para feixes não planares. A análise gama dos planos de IMRT e VMAT revelou pequenas diferenças na exactidão do cálculo com e sem FF.

Conclusão: Os resultados mostraram que é possível desenvolver planos clinicamente aceitáveis para IMRT e VMAT, com e sem FF. O conceito de *Pareto optimal fronts* revelou-se um método eficaz para comparar diferentes métodos e diferentes técnicas avançadas de Radioterapia.

Palavras Chave: *Flattening filter*, *Cancro da Prostata*, *IMRT*, VMAT, *Pareto Optimal Fronts.*

Abstract

Purpose: The interest of linear accelerators operating without flattening filter (FF) has been increasing in the last few years. For this reason the study of the treatment plan quality delivered with and without FF (FFF) is the aim of this project.

Materials and methods: For this study three early stage prostate cancer cases were selected. A treatment planning study based on the concept of Pareto optimal fronts, which is considered to provide a more scientific approach, was performed. Several plans were made for Intensity Modulated Radiotherapy (IMRT) and Volumetric Modulated Arc Therapy (VMAT) with and without FF. By systematically varying the EUD maximum of a specific OAR, different dose distributions have been calculated.

Pareto optimal fronts to compare the two delivery techniques were evaluated. The Pareto fronts were determined by plotting presentable values of the dose distribution of the planning target volume (PTV) and the organs at risk (OAR). Comparing the fronts of each delivery technique will help to decide whether one technique is superior to the other.

Results: Plans with similar plan quality were generated for IMRT and VMAT with flattened and unflattened beams. For the case 1 and 2 the Pareto optimal fronts differed significantly for IMRT and VMAT, in favor for IMRT. For the third patient, the fronts laid virtually on top of each other. The number of MUs was 9-15% higher for unflattened beams. By the use of FFF the treatment time was reduced by 24% for IMRT FFF and decreased even further for both VMAT techniques. The γ index evaluation of the IMRT and VMAT plans showed little difference in calculation accuracy in FFF mode compared with the regular beam.

Conclusion: The results showed that is possible to develop clinically acceptable plans for IMRT and VMAT, with flattened and unflattened beams. The approach of using Pareto fronts for different systems is a feasible way to compare different methods and techniches for advanced radiotherapy.

Keywords: Flattening filter, Prostate Cancer, IMRT, VMAT, Pareto optimal fronts.

Contents

List of Tables

List of Figures

List of Abbreviations and Acronyms

2D	Two dimensional
3D	Three Dimensional
CT	Computed Tomography
DICOM	Digital Imaging and Communications in Medicine
DTA	Distance-to-agreement
DVH	Dose-Volume Histogram
Eq	Equation
EUD	Equivalent Uniform Dose
FF	Flattening Filter
FFF	Flattening Filter Free
Gy	Gray
ICRU	International Commission on Radiation Units and Measurements
IMRT	Intensity Modulated Radiotherapy
J	Joule
LCS	Linac Control System
MeV	Mega electron-volt
MLC	Multileaf collimator
MO	Missouri, USA
MU	Monitor Unit

MUW	Medical University of Vienna
MV	Mega voltage
NT	Normal Tissue
NTCP	Normal Tissue Complication Probability
OAR	Organ at risk
PMMA	Polymethyl Methacrylate
PTV	Planning Target Volume
QA	Quality Assurance
QUANTEC	Quantitative Analyses of Normal Tissue Effects in the Clinic
RT	Radiation Therapy
SI	International System of Units
SRS	Stereotactic Radiosurgery
TCP	Tumor Control Probability
TPS	Treatment Planning System
VMAT	Volumetric Modulated Arc Therapy
UK	United Kingdom
XVMC	X Voxel Monte Carlo

1 Introduction

Medical linear accelerators (Linacs) are usually equipped with flattening filters[1] to compensate for the non-uniform energy fluence distribution of the photons generated in the target.

Recent studies have shown various advantages of Linacs operated without flattening filters[2-9]. One advantage is an increased dose rate, which is beneficial for the patient due to a reduction of treatment time[10]. Furthermore, the removal of the flattening filter (FF) leads to a reduction of head scatter, leaf transmission and leakage radiation.[11,12] These properties result in a reduction of the patients' exposure to peripheral dose at large distances from the edges of the treatment field.

Due to the conical shape of flattening filter a decrease of the average energy of the photon beam with increasing distance from the central axis can be observed.[13] Since this so called off-axis softening is less pronounced when the flattening filter is removed similar or even higher dose calculation accuracy can be expected from unflattened beams.

Vassiliev *et al.*[3] have shown that it is possible to generate IMRT treatment plans for flattened an unflattened beams which are dosimetrically similar. For the unflattened plans, however, a reduction of the beam-on time and monitor units (MUs) was observed.[3,6] While current sequencing algorithms are not customized for non-uniform beams and therefore lead to a high number of segments, Kim *et al.*[14] developed an algorithm which is able to reduce the number of segments significantly for treatment plans with unflattened beams.

The aim of this thesis is to determine the feasibility of developing clinically acceptable treatment plans using unflattened beams, compare them with typical plans developed with flattened beams, and explore the potential benefits and drawbacks of using unflattened as opposed to flattened beams. Two types of treatment plans will be investigated: Intensity Modulated Radiotherapy (IMRT) and Volumetric Modulated Arc Therapy (VMAT). As sequencing is a vital step in producing treatment plans by inverse planning, the ability of the sequencer to handle unflattened beams is of special interest.

An Elekta Precise® Linac (Elekta AB, Stockholm, Sweden) at the Medical University of Vienna (MUW) was modified to deliver flattened and unflattened photon beams. In the flattening filter free (FFF) mode of the accelerator a copper disk is rotated into the

beam line instead of the flattening filter to ensure beam stability.[13] The Linac is equipped with multileaf collimators (MLC) of MLCi type (40 leaf pairs). Basic beam data was acquired and implemented into Monaco™ (Elekta CMS Software, St. Louis, MO).

The initial step of this study is to determine whether the Treatment Planning System (TPS) Monaco™ is able to create clinical acceptable plans for IMRT and VMAT with and without FF.

Three prostate cancer patients previously treated with IMRT at the MUW were selected. One plan per investigated treatment modality for each patient was produced. Their characteristics are determined by analyzing the dose-volume-histograms (DVHs) of the planning target volume (PTV) and the organs at risk (OARs). Certain values, e.g. target-coverage, -conformity and –homogeneity, in the PTV, as well as maximum dose in the OARs, are derived from the DVHs.

By systematically varying the serial cost function of the rectum, different dose distributions were calculated. Pareto optimal fronts were created. Comparing the fronts of each delivery technique will help to decide whether one technique is superior to the other.

The treatment time (T) was recorded and evaluated by delivering the four initial plans of each patient using Elekta Precise® Linac (Elekta AB, Stockholm, Sweden), modified for the application of FFF beams.

Finally, dosimetric accuracy of IMRT and VMAT plans with and without flattening filter have been assessed by measurements with a 2D detector array Delta4™ (ScandiDos, Upsala, Sweden), which also allows a quasi-3D dose acquisition. The acquired data was analyzed by gamma index analyses as proposed by Stock *et al*.[15]

This thesis consists of 6 chapters.

After the introduction given in Chapter 1, in Chapter 2, the basic fundamentals of this project are explained. This includes the Linear Accelerator, the flattening filter, quantities that were used, the modulated techniques, Monte Carlo methods, equivalent uniform dose formalism and the Pareto Optimality concept.

Chapter 3 describes the background and the motivation of this work, the characterization of the linear accelerator, the beam properties of flattening filter free, the IMRT and VMAT techniques, the Monte Carlo Algorithm and the radiobiological models.

In chapter 4 the materials and methods applied in this project are fully described, as the clinical cases selected, the planning process, the plan evaluation, the Pareto optimal fronts creation and the plan measurements.

In chapter 5 the summary of the results obtained from the project are described and discussed: the treatment plans produced for the three patients are presented. The Pareto optimal fronts generated for each patient are shown, and based on that fronts the IMRT and VMAT techniques with and without flattening filter are compared. The time required to deliver the initial plans of each patient is listed and compared. The initial plans were measured and the response of the dosimetry equipment was compared with the calculated dose matrices by gamma evaluation.

2 Fundamental concepts

2.1 Medical linear accelerator

Medical linear accelerator (Linac) is an equipment that uses high-frequency electromagnetic waves to accelerate charged particles, such as electrons, to high energies trough a linear tube. These electrons can be extracted from the unit and used for the treatment of shallow lesions, or they can be directed to a target to produce high-energy x-rays for treatment of deep-seated tumors.[16]

2.2 Flattening Filter

Flattening filter, usually with a conical shape, are made of medium and/or high Z materials and are shaped to produce a field of uniform intensity at a specified depth.[17]

2.3 Absorbed dose

The absorbed dose is defined as the amount of energy deposited in a medium by ionizing radiation per unit mass.[18]

Formally, absorbed dose at a point is defined by the ICRU as

$$\mathrm{D} = \frac{\Delta \mathrm{E}}{\Delta \mathrm{m}}$$

(eq. 1)

where ΔE is the mean energy transferred by the radiation to a mass Δm.

The SI unit of absorbed dose is gray (Gy) and is defined as the absorption of 1 J of energy per kilogram of medium.

2.4 Dose Rate

Dose Rate is the rate of energy absorption per unit mass in a defined point.[19] In SI units, dose rates may be expressed as Gy/s, mGy/h, etc., and because the Gy is such a large unit compared to many common circumstances, the unit Gy/h is often used.

2.5 Photon Fluence

The photon fluence Φ is defined as the quotient dN by dA,[20] where dN is the number of photons that enter in an imaginary sphere of cross-sectional area dA:

$$\Phi = \frac{dN}{dA}$$

(eq. 2)

The unit of photon fluence Φ is cm^{-2}.

2.6 Output factor in air

The in-air output ratio, S_c, is defined as the ratio of primary collision water kerma in free-space, K_p, per monitor unit between an arbitrary collimator setting and the reference collimator setting at the same location.[21]

Output factor in air is most commonly called collimator scatter factor or head scatter factor. Measurements and analytical studies have shown that there are multiple components for output factor in air, in particular, photon head-scatter inside accelerator head, x-ray source obscuring effect, and monitor backscatter effect. Various sources of head-scatter, which include the flattening filter (and a wedge, if used), have been characterized.

2.7 Intensity Modulated Radiation Therapy

IMRT is the delivery of radiation to the patient via fields that have non-uniform radiation fluence.[22] It is a sophisticated type of three-dimensional conformal radiotherapy that assigns non-uniform intensities to a tiny subdivision of beams called beamlets. The ability to optimally manipulate the intensities of individual rays within each beam leads to greatly increased control over the overall radiation fluence.

2.8 Volumetric modulated arc therapy

Volumetric modulated arc therapy is a technique that delivers a precisely sculptured 3D dose distribution with a single 360-degree rotation of the linear accelerator gantry. This is possible by a treatment planning algorithm that simultaneously changes three

parameters during treatment: (1) rotation speed of the gantry, (2) shape of the treatment aperture using the movement of multileaf collimator and (3) delivery dose rate.[23]

2.9 Monte Carlo method

The Monte Carlo (MC) method is a stochastic method for solving complex equations providing approximate solutions by performing statistical sampling experiments on a computer. They are based on the use of pseudo random numbers and probability statistics to investigate problems.[24,]

These methods derive their collective name from the fact that Monte Carlo, the capital of Monaco, has many casinos and casino roulette wheels are a good example of a random number generator. [25,26]

The Monte Carlo simulation techniques have formally existed since the early 1940s, where it had applications in research into nuclear fusion. Nowadays MC methods are widely used to solve complex physical, economical and mathematical problems, to regulate the flow of traffic, etc.

In particle transport the Monte Carlo technique is used to simulate a huge number of histories of individual photons and electrons including all daughter particles. Probability distributions are randomly sampled using transport data to determine the outcome at each step of its life.[27]

2.10 Equivalent Uniform Dose

The concept of Equivalent Uniform dose (EUD) for tumors was introduced by Niemierko[28] originally as the biologically equivalent dose. For any dose distribution, the corresponding EUD is the dose in Gy, which, when distributed uniformly across the target volume, causes the survival of the same number of clonogens. Later, Niemierko extended the EUD concept to apply to normal tissues as well.

2.11 Pareto optimality

The Italian economist Vilfredo Pareto introduced the mathematical concept of Pareto optimality, a concept that formalizes the trade-off between a given set of mutually contradicting objectives.[29,30]

A solution is said to be Pareto optimal when it is not possible to improve one objective without deteriorating at least one of the others. A Pareto front is constituted by the Pareto optimal solutions (see figure 1). This concept can be used as an optimization method, but also as an analytical instrument.

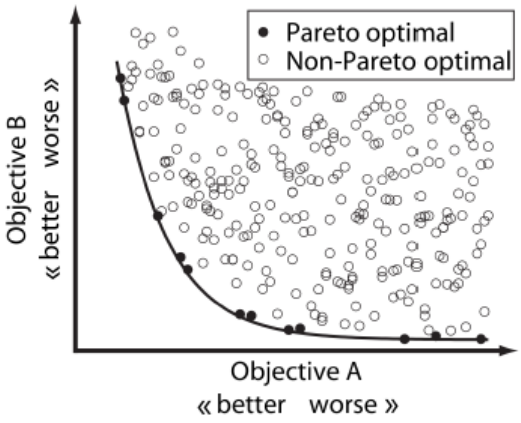

Figure 2.1 The Pareto concept for a given optimization problem. With two mutually contradicting objectives an infinite number of solutions exist. All Pareto optimal solutions build the Pareto front.[31]

3 Background

In external radiotherapy, the x-ray treatment fields are usually delivered by a medical linear accelerator. Various types of modern linear accelerator designs are available.

The Linac can be used in two distinct operation modes: electron mode and photon mode. In electron mode primary electrons are used for treatment, in photon mode, photons are produced for treatment.[32]

In photon mode primary electrons are directed onto a bremsstrahlung target. This target creates bremsstrahlung radiation with a thin tungsten disk of approximately 1 mm height.

The high-energy x-ray beam produced in the target is defined by a primary collimating system and is intercepted by a flattening filter and multiple ion chambers before exiting the head of the machine through a secondary collimator consisting of movable leaves.[33]

The flattening filter is placed in the x-ray beam to reduce the intensity of the forward peaked dose in the center of the field.[17]

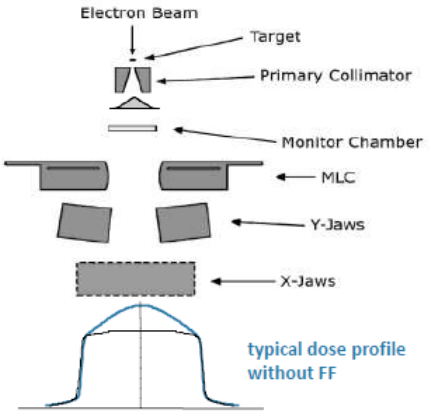

Figure 3.1. Schematic cross section of the treatment head of an Elekta Linac and typical dose profile without FF.[35]

Metcalfe *et al*[36] referred that to be useful for conventional radiotherapy the treatment fields have to be uniform. This 'beam flatness' was achieved by the introduction of a flattening filter in the beam line.

With the advent of IMRT and other modulated techniques, the original photon fluence will be modified by the movement of the MLC, therefore questions the need for a FF.[37]

3.1 Beam properties of unflattened beams

There are several studies that summarize the dosimetric properties of unflattened photon beams based on Monte Carlo (MC) simulations or dosimetric measurements.[35,38-48] These studies have shown many advantages in removing flattening filter from the beam line. Recently, Kragl *et al*[45], Cashmore[4] and Dalaryd *et al*[48] have published experimental data on the dosimetric characteristics of unflattened beams.

The main advantages of removing the flattening filter are an increased dose rate[4,39,45], which is beneficial for the patient due to a reduction of treatment time[11], reduced scatter[4,42,45], reduced leaf transmission and leakage radiation[4], reduced out of field doses[48] and reduction in the dose from neutrons to the patient and to radiation personnel[2,49,50].

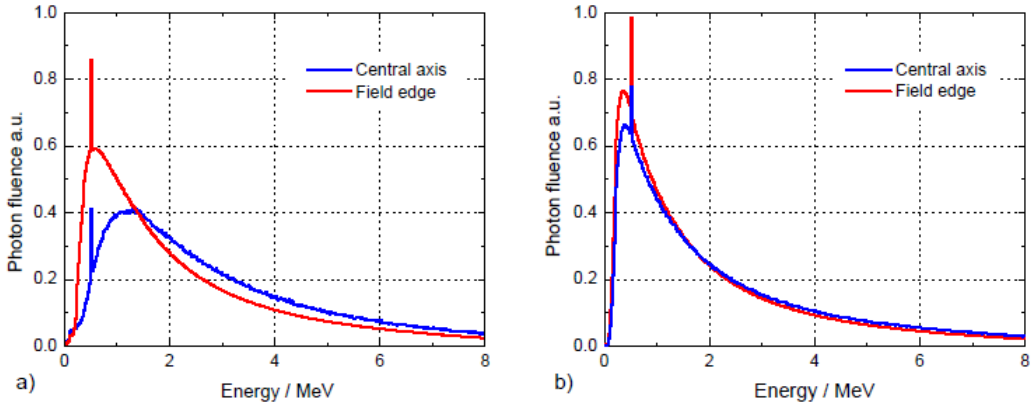

Figure 3.2. Comparison of Monte-Carlo simulated X-ray spectra on the central beam axis and the field edge of a) flattened and b) unflattened 10 MV beams provided by an Elekta Linac.[47]

Figure 3.2 shows unnormalized Monte-Carlo simulated X-ray spectrum of flattened and unflattened 10 MV beams provided by an Elekta Linac. From Figure 3.2 two effects become apparent. Firstly, the photon energy fluence for FFF beams is increased and results in an increased dose per pulse[47], as mentioned above. Secondly, the off-axis spectral dependence is very small, based on this we can expect a similar or even higher dose calculation accuracy for unflattened beams.

3.2 IMRT/VMAT

IMRT is the delivery of radiation to the patient via fields that have non-uniform radiation fluence.[37]

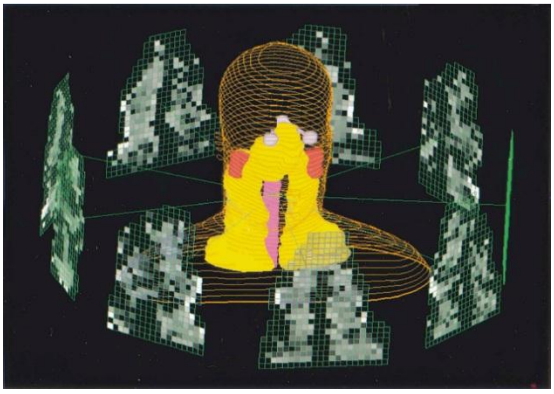

Figure 3.3. An example of a 9 field IMRT technique dose distributions, where the grey levels indicate the intensity values of the beamlets.[51]

Several papers have addressed this issue of unflattened beams for IMRT.[3,8-10] In theory, the flattening filter could be removed and the required fluence distribution can be achieved by modulating the unflattened non-uniform fluence distribution directly.[4,10]

The current method of optimizing the photon beam fluence using MLCs is realized by manipulating the uniform photon beam fluence by creating areas of high and low intensity according to the requirements of the plan. The photon beam fluence is divided into elemental beam areas that are assigned a weight which is directly proportional to the MU that will be delivered through this area (segment). The weights of each elemental area are then manipulated (increased or decreased) with respect to its contribution to the planning dose criteria. The optimized beam intensity is then delivered using the MLC. Several beam segments of different MUs are used in each case to deliver the planned photon fluence. Since the photon beam fluence is based on the optimization of elemental areas, it is not conceptually necessary to start with a uniform beam[8].

The reduction of treatment head leakage and scattered radiation for FFF beams is advantageous for IMRT.[17] Although the increased dose rate of FFF beams is another potential advantage for IMRT, the MU delivery is only one contribution to the total time for a treatment fraction. The reduction of beam-on time may be discounted by the increase of leaf-travel time and (or) verification-and-recording time.[10]

For segmental or step-and-shoot IMRT, the number of segments and, consequently, the leaf travel time has a large impact on treatment delivery efficiency, especially for standard fractionation schemes with about 2 Gy per fraction. When using the same objectives for treatment plan optimization, it cannot be *a priori* assumed that the number of segments is identical for IMRT plans with and without FF.[17]

While current sequencing algorithms are not customized for non-uniform beams and therefore lead to a high number of segments, Kim *et al.*[52] developed an algorithm which is able to reduce the number of segments significantly for treatment plans with unflattened beams.

Stathakis *et al*[8] reported a significant reduction in the number of MUs for several IMRT indications. However, the Linac was calibrated to provide doses of 2 cGy and more than 3 cGy per MU for 6 and 18 MV beams without a FF. When using a standard Linac calibration of 1 cGy/MU, the total number of MU will probably be very similar for flattened and unflattened beams. For sliding window IMRT and rotational IMRT, the current leaf speed around 3 cm per second has a natural limit for the dose rate.[17]

During the last years rotational IMRT or VMAT has become a promising and commercially available treatment option.[23,54,55]

VMAT is a completely dynamic technique performed by means of one or more gantry arcs: while the gantry is rotating beam aperture is changed continuously, the dose rate is varied and collimator rotation is also enabled. Treating the patients with the widest number of beam orientations may potentially ensure high dose conformity and sparing of normal tissue reducing simultaneously the number of MU and delivery times with respect to other established modulating techniques.[55]

Unflattened beams provide a larger dose rate range, which might offer advantages in the optimization of rotational IMRT. Finally, unflattened beams might be more stable during delivery of static or rotational IMRT since they are less susceptible to changes in beam steering.[4,17,47]

3.3 Treatment Planning System

Current cancer treatment techniques as IMRT and VMAT allow precise dose deposition in the target volume and an improved spare of the normal tissue. A good plan and accurate dose calculation is essential to assure the efficacy of these techniques.

3.3.1 Dose Calculation Algorithms

For many years Monte Carlo is a commonly known dose calculation algorithm for researchers in the field of radiotherapy, since it represents the most accurate method for absorbed dose calculations.[56] However, the implementation of Monte Carlo calculations in clinical use are time consuming and need high performance computing to be time efficient and practical. To reduce the calculation times Fippel *et al.*[57] developed a fast Monte Carlo algorithm for photon beams called XVMC.

The implementation of this algorithm is important to solve the central problem of IMRT, the modelling of radiation transport through complex geometries. Field geometries are much more irregular and smaller in IMRT than in conventional radiotherapy. With smaller field sizes, the modelling of scatter from the collimators or compensator filters becomes more important. These effects can be modeled precisely with Monte Carlo methods.[58] The simulation of radiation transport with these methods imitates the physical processes at the price of significantly longer computation times. Nevertheless, Monte Carlo dose computation was included into the algorithm with clinically acceptable computation times.[59]

The dose calculation algorithms implemented in the treatment planning system (TPS) Monaco™ (Elekta CMS Software, St. Louis, MO) are Pencil kernels and Monte Carlo. Figure 3.4 illustrates exemplarily that Monaco™ with multi-source models and advanced dose calculation algorithms can be commissioned for FFF beams.

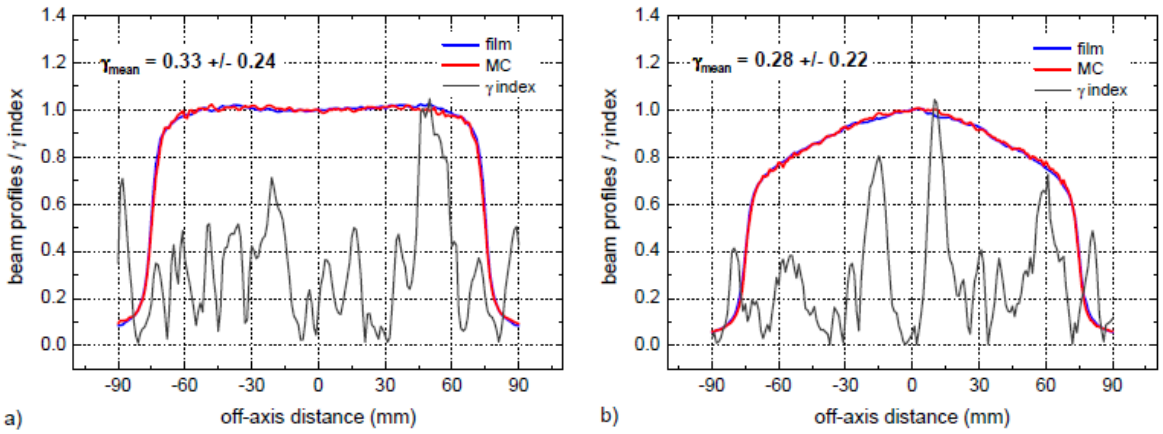

Figure 3.4. Comparison of measured and MC-calculated profiles of a) flattened and b) unflattened 10 MV beams obtained during commissioning of the TPS Monaco™, for a 15 x 15 cm^2 field at 10 cm depth. Courtesy of Elekta.

3.3.2 Optimization incorporating biological information

The goal of radiation therapy is to maximize tumor response while minimizing side effects in normal tissues. Optimization of treatment plans has traditionally been performed using surrogate approaches, such as maximization of tumor dose and minimization of dose to organs at risk.[60]

Many studies demonstrated that incorporating biologically based objective function, which takes patient and tumor/organ-specific biological features, into inverse treatment planning algorithms can substantially improve the quality of the plan generated leading to improve sparing of organs at risk with comparable target coverage.[60-65]

A number of mathematical models have been developed over the years to better describe the biological effect of radiation, which include tumor control probability (TCP),[66] normal tissue complication probability (NTCP),[67] equivalent uniform dose (EUD)[28] and the probability of uncomplicated tumor control (P+).[68,69]

The optimization based on radiobiological models became even more important with the advent of IMRT and inverse treatment planning,[70,71] although the progress was hampered by limitations of plan optimization based on purely biological indices.[72]

An equivalent uniform dose concept[28,73] has gained considerable popularity in the area of biologically based treatment planning because it incorporates information about the organ functional architecture (serial or parallel), lies in a more familiar to clinicians dose-volume domain, and possesses desired mathematical properties.[61,74] At the moment, does not rely on too many parameters with large uncertainties, such is the case with TCP and NTCP.

The concept of Equivalent Uniform Dose (EUD) for tumors was introduced by Niemierko[28] originally as the biologically equivalent dose that, if given uniformly, would lead to the same cell kill in the tumor volume as the actual non-uniform dose distribution. Later, Niemierko[73] extended the EUD concept to apply for both tumors and normal tissues.

$$EUD = \left(\frac{1}{N}\sum_{i} D_i^a\right)^{\frac{1}{a}}$$

(eq. 3)

In this expression, N is the number of voxels in the anatomic structure of interest, D_i is the dose in the i'th voxel, and a is the tumor or normal tissue-specific parameter that describes the dose–volume effect. This formulation of EUD is based on the power law dependence of the response of a complex biologic system to a stimulus. This type of relationship has been observed in many biologic phenomena since the mid-19th century and has also been incorporated into the EUD concept.

EUD described in Eq. 1 is the general mean of the non-uniform dose distribution. According to the mathematical properties of the function[75] for $a=\infty$ the EUD is equal to the maximum dose, and for $a= -\infty$, the EUD is equal to the minimum dose. Tumors generally have large negative values of a, whereas serial critical structures (e.g., spinal cord and rectum) have large positive values and parallel critical structures that exhibit a large dose-volume effect (e.g., liver, parotids, and lungs) have small positive values.

The simplicity of EUD is due in part to the fact that the same formalism is used for both tumors and normal tissues and in part that the desired EUD values can be easily related to conventionally required dose or dose–volume limits.

Many investigators have demonstrated that incorporating EUD based or hybrid, EUD and dose-based, cost functions into inverse treatment planning algorithms often leads to improved sparing of OARs with comparable target coverage.[61,76-79]

The biological cost functions implemented in the Monaco™ are based on a formalism developed at the University of Tübingen,[59,80] which is comprised of sparsely parameterized expressions to convert three-dimensional dose distributions to either an EUD for the Poisson cell kill model and Serial complication model or a fraction of organ damaged for the Parallel complication model. These biological indices are then included in the overall objective score for plan optimization.

3.4 Motivation

The interest of a linear accelerator operating without flattening filter has been increasing in the last few years. The flattening filter (FF) was considered as an essential component of almost all linear accelerators, acting to produce a flat beam from the forward-peaked photon fluence produced at the target.

With the introduction of IMRT, the initial flat beam is no longer needed since the required fluence distributions can be achieved by modulating the unflattened non-uniform fluence distribution directly.

Besides that, recent studies have reported various advantages of removing the flattening filter. The major advantages are an increased dose rate[3], reduced scatter, reduced leakage and reduced out-of-field doses.

The benefits of unflattened beams are already reported in the community however, before implementing these techniques without FF in a clinical environment, treatment planning studies must be done, in order to evaluate the ability of the TPS to handle unflattened beams.

The motivation for this work is related to the possibility to perform IMRT/VMAT treatments without flattening filter reducing the peripheral doses in the patient and reducing the treatment time.

4 Materials and Methods

4.1 Linear Accelerator

All measurements in the framework of this thesis were performed with an Elekta Precise® Linac (Elekta AB, Stockholm, Sweden) at the Medical University of Vienna (MUW) that was modified to deliver flattened and unflattened photon beams. In the FFF mode of the accelerator a 6 mm thick copper disk (fig. 4.1) is rotated into the beam line instead of the flattening filter to ensure beam stability. The beam servo control and feedback system to electron gun, which is driven by the monitor chamber in the particular Linac, could thus be operated in a quasi-clinical mode. To prevent unflattened beams from accidental clinical use the Linac Control System (LCS) for FFF beams was running on a separate hard drive.

The Linac is equipped with an MLC consisting of 40 leaf pairs (isocentric leaf width 1 cm) and backup-jaws allowing a maximum field size of 40 x 40 cm^2.

a) b)

Figure 4.1. The cooper filter used in FFF mode a) and the carousel of an Elekta Linac b). Courtesy of Elekta.

The calibration of the linear accelerator for the 10 MV energy was performed to have 1 cGy/monitor unit (MU) for a 10 x 10 cm^2 field at a depth of 10 cm.

4.2 Treatment planning system

Treatment plans were performed with the Treatment Planning System CMS Monaco™ version 2.04 (Elekta CMS Software, St. Louis, MO) – non-clinical version.

Monaco™ is one of the first commercial IMRT treatment planning systems based on biological optimization. In addition to physical cost functions, such as dose-volume

histogram (DVH) constraints and maximum dose, Monaco^{TM} offers three biological cost functions.

Monaco^{TM} 2.04 optimizes the dose distribution in the PTV and OARs by assigning one or more cost functions to each structure and minimizing these cost functions.

A summary of cost functions used to design the Monaco plans is shown in Table 4.1. For each cost function assigned to a structure, the TPS computes an index that reflects presumed biological response of the structure to a currently attained dose distribution. This index is referred as isoeffect, and depending on the type of cost function may be expressed either in units of dose or as a percentage of organ damaged.

Following each optimization step, calculated isoeffects for all cost functions were compared with user-specified values referred to as isoconstraints. Optimization is stopped when no additional dose can be given to targets without isoeffects exceeding their corresponding isoconstraints.

Table 4.1 Cost functions used to design Monaco plans[81]

Applicability	Model name	Parameters and isoconstraints	Description
Biological cost functions			
Targets	Target EUD	Cell sensitivity (0.1–1.0) EUD prescription (Gy or cGy)	Mandatory cost function for targets; no penalty for hot spots
OARs	Serial	Power law exponent (≥1) Equivalent uniform dose (Gy or cGy)	Penalizes for hot spots
OARs	Parallel	Reference dose (Gy or cGy) Power law exponent (≥1) Mean organ damage (%)	Effective for reducing mean organ dose
Physical cost functions			
Targets or OARs	Quadratic overdose penalty	Maximum dose (Gy or cGy) Root mean square dose excess (Gy or cGy)	Penalizes for hot spots with some leniency
Targets or OARs	Maximum dose	Maximum dose (Gy or cGy)	Penalizes for hot spots with zero leniency

OARs	Overdose-volume DVH	Threshold dose (Gy or cGy)	Forces a DVH through or below a single point

4.2.1 Optimization Process

Monaco™ employs a two-stage process for the optimization of dose distributions. The TPS optimizes the dose distribution in the PTV and OARs by assigning one or more cost functions to each structure, in agreement with the dose prescriptions, and minimizing these cost functions[58].

In the first stage the optimized fluence maps are created and the dose distribution is calculated with a finite size pencil beam algorithm.[82] In the second stage, the beam segmentation is optimized. The sequencer tries to rebuild these fluence maps by optimizing the number and shape of the segments for each beam. This is done by varying the shape of the segments, updating the dose distribution by Monte Carlo simulation and recalculating the optimization problem[59]. This process is repeated till an improvement of the optimization can be no longer observed.[81]

The plans were made for delivery on an Elekta Precise® linac (Elekta AB, Stockholm, Sweden) which use the Elekta MLCi beam shaping.

4.3 Dosimetric equipment

The dosimetric accuracy of IMRT and VMAT plans with and without flattening filter have been assessed by measurements with a 2D detector array (Delta 4 by ScandiDos), which also allows a quasi-3D dose acquisition. The acquired data was analyzed by gamma index analyses as proposed by Stock et al.[15]

4.3.1 Delta 4

The Delta 4 phantom (Scandidos, Uppsala, Sweden) consists of a crossed array inside a 22 cm diameter cylindrical polymethyl methacrylate (PMMA) phantom, and associated computer software allows the user to compare the measured dose distribution for a complete treatment plan with the dose distribution predicted by the treatment planning system.[83]

There are a total of 1069 *p*-type cylindrical silicone diodes, which active volume is 1 mm in diameter and 0.05 mm thick. The nominal detector sensitivity is 5 nC/Gy. Temperature sensitivity variation is reported by the manufacturer as 0.32%/°C.

The detectors are arranged in rectangular patterns on two orthogonal planes. The first plane is called the “main board” and has the measurement area of 20 × 20 cm^2. The other plane is made up of two halves (“wings”), covering 20 × 10 cm^2 each, which allows easy assembly of the detector boards in the orthogonal position in the phantom. The central line of detectors on the main board coincides with the long axis of the phantom.

The detectors are spaced 0.5 cm apart in the central 6 × 6 cm^2 area, and 1 cm apart elsewhere. Rather than being angled ± 45º, the detector boards are separated from the vertical by + 50° (main board) and - 40º (wings). The phantom can be positioned on the couch with the electrometers facing either away from the gantry (Fig. 4.2), or towards the gantry (reversed orientation).

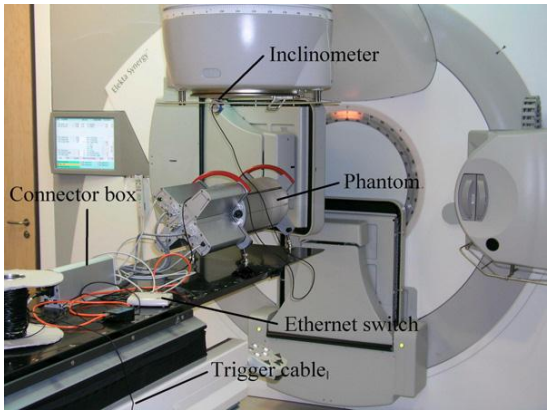

Figure 4.2. The Delta4 phantom and associated devices positioned on the Linac couch.[84]

The device records measured dose in relation to the individual accelerator pulses by using a trigger signal from the accelerator. The trigger pulse precedes the dose pulse by a few microseconds. Readings over several dose pulses are packaged and sent to the control PC. This synchronization of the measurement with the accelerator pulse improves the signal to noise ratio, and adds the temporal dimension to the data, allowing, for example, the association of the dose-packages with individual control points (segments) of the IMRT plan. For rotational treatments, gantry angle is independently sensed by means of an inclinometer attached to the gantry or

accelerator head. This allows the device to identify which control point of a dynamic arc delivery is being delivered, so that the measured dose can be associated with this control point and the appropriate correction for gantry angle applied.[85]

4.3.1.1 Delta 4 calibration

The Delta 4 phantom needs to be calibrated by the user once a year.[83] The unit is equipped with a calibration PMMA phantom, to perform the calibration. The relative calibration (equalization), establish the basic sensitivity value for each diode detector relative to the reference detector, and the absolute dose calibration is performed to convert the detector signal in absolute dose values.

4.3.2 Ionization chamber

An ionization chamber consists of a gas filled cavity between two conducting electrodes. When the gas between the electrodes is ionized, the produced ions and dissociated electrons move to the electrodes of the opposite polarity, thus creating ionization current. This current can be amplified and measured. There are multiple designs of ionization chambers. For dose determination in water, the most common types are cylindrical chambers with air as counting gas. They consist of an active volume with a central collecting electrode, located in the axis of symmetry. Typically, the active volume of an ionization chamber in medical use ranges from 0.1 cm^3 to 1 cm^3.[86]

An ionization chamber PTW 31003 (Farmer type chamber) with an active volume of 0.6 cm^3 was used for measure the Linac daily output.

4.4 Prostate cases

For this study three early stage prostate cancer cases were selected from a database of patients previously treated with IMRT at the Medical University of Vienna. The selection criteria for the cases were: PTV, rectum, bladder, left and right femoral heads and normal tissues fully delineated, and an overlapping of the target with the rectum. As a result of this overlap it is expected to be a conflict or trade-off in the optimization between the overlapping structures. The PTV includes the prostate plus 5mm uniform margin. The rectum was filled with a rectum balloon and the bladder of the three

selected patients have more than 152 cm^3. More details on the cases are given in table 4.2.

Table 4.2 Case specific information

	Prescription (Gy)	**Prostate** (cm^3)	**PTV** (cm^3)	**Rectum** (cm^3)
Prostate 1	78	28	106	119
Prostate 2	78	73	202	109
Prostate 3	78	65	185	100

4.5 IMRT/VMAT planning

In order to evaluate the possibility to create clinical acceptable treatment plans to deliver with flattened (FF) and unflattened beams (FFF), treatment plans for IMRT and VMAT were produced, for each patient.

For IMRT the prescription dose was 78Gy in 2Gy fractions to the PTV. A target EUD cost function was applied to the target, and a serial cost function has been applied to the rectum and to the bladder. A constraint was applied to the normal tissue to prevent for non-allowed hot spots. Nine coplanar and non- opposing beams of 10 MV photons were used for the IMRT planning with step-and-shoot delivery. The gantry was placed at 180º, 220º, 260º, 300º, 340º, 20º, 60º, 100º and 140º.

For VMAT one full arc of 360º (from -180º to 180º) of 10 MV photons was planned without gaps in delivery. The prescription dose was 78Gy in 2Gy fractions to the PTV. The same cost functions and OAR dose constraints have been applied.

In order to create similar plans for IMRT and VMAT the “rule of 3” proposed by Elekta have been applied,[81] this means that the user should add three (3) to the number of static beams that he used to treat this patient. For example, if nine (9) beams were used to plan a standard IMRT plan, consider creating 12 sectors (9+3) for VMAT. 360 deg arc/12sectors = increment of 30.

In this case 5 beams IMRT plans and a full VMAT arc with 12 sectors were created. In order to create similar plans 4 beams were added to the IMRT plans, in total, 9 beams have been created for IMRT technique with and without FF.

Dose distributions have been calculated using the Monte Carlo algorithm with 3% Monte Carlo variance. The calculation grid was 3mm.

4.6 Plan evaluation

The characteristics of the plan have been determined by analyzing the dose-volume-histograms (DVHs) of the planning target volume (PTV) and the organs at risk (OARs). The treatment plans have been considered as clinically acceptable if 95% of the PTV volume receive more than 95% of the prescribed dose and if fulfill the QUANTEC recommendations for OAR. For the rectum[87]: V_{50}<50%, V_{60}<35%, V_{65}<25%, V_{70}<20%, and V_{75}<15%. For the bladder[88]: V_{15}<80Gy, V_{25}<75Gy, V_{35}<70 Gy and V_{50}<65Gy.

4.7 Pareto Optimal Fronts

The second step of this study was to determine whether the treatment planning system Monaco™ (Elekta Oncology Systems) can be used to obtain Pareto optimal fronts.

Pareto optimality is a concept of formalizing the trade-off between contradicting objectives of a given optimization problem.

The Pareto concept applies well to the inverse planning process in which more than one objective function has to be optimized simultaneously.[89,90]

Ottosson *et al.*[31] have shown the feasibility of planning studies using Pareto fronts and successfully used it to compare different dose calculation algorithms for different photon beam energies.[91]

In this study, Pareto fronts were created for prostate cases by varying the EUD maximum for the rectum. The plan was rejected when the coverage of PTV was compromised. The target coverage is expected to decrease with the decrease of the EUD maximum for the rectum.

The number of plans produced for each patient per treatment modality, is listed in table 4.3. For the first patient 191 plans were created by systematically varying the EUD maximum for the rectum, and for four fix values of EUD maximum of the bladder. After to create such a big number of plans, the fronts were created and it was noticed that it have a lot of non-Pareto optimal plans. For this reason it was decided to reduce the number of plans for the next patients. For the second and the third patients the number

of plans was reduced to 76 plans and 75 plans, respectively. As in the first patient the plans were created by systematically varying the EUD maximum for the rectum (until the plan been rejected) and for two fix values of the EUD maximum of the bladder.

Table 4.3 Number of plans produced for each patient per treatment modality

	IMRT FF	IMRT FFF	VMAT FF	VMAT FFF
Patient 1	*46*	*44*	*50*	*51*
Patient 2	*19*	*20*	*19*	*18*
Patient 3	*19*	*20*	*18*	*18*

The dose of the most exposed 10% of the rectum (D10%) was used together with the volume of the PTV which received less than 95% of the prescribed dose (100%-$V_{95\%}$PTV/%) to comprise the fronts. Rectum sparing was chosen as an evaluation parameter for the prostate cases as it competes with PTV coverage.

For each patient and technique the DVH's generated by Monaco were exported and imported in MATLAB R2009b (The MathWorks, Inc., Natick, MA, USA) to plot the fronts. The fronts were generated and compared for each technique and for each patient. The points not contributing to the front were discarded. Comparing the fronts of each delivery technique will help to decide whether one technique is superior to the other.

4.8 Doses, Segments and Treatment Times

The near maximum ($D_{2\%}$), near minimum ($D_{98\%}$) and median dose ($D_{50\%}$) were reported for the PTV according to ICRU 83 recommendations. Also, the number of monitor units (MUs) and segments (Seg) were recorded.

The treatment time (T) was evaluated by delivering the four initial plans of each patient using Elekta Precise® Linac (Elekta AB, Stockholm, Sweden), modified for the application of FFF beams.

4.9 Conformity Index and Homogeneity Index

The conformity index (CI) and homogeneity index (HI) were computed to assess the quality of the dose distribution.

The Dose conformity index used in this work was introduced by van't Riet, *et al*.[92] and simultaneously takes into account the irradiation of the target volume and the irradiation of healthy tissues, and is defined as:

$$CI = \frac{TV_{RI}}{TV} x \frac{TV_{RI}}{V_{RI}}$$

(eq. 4)

where TV_{RI} is the target volume covered by the reference isodose, *TV* is the target volume, and V_{RI} is the volume of the reference isodose.

The first fraction of this equation defines the quality of coverage of the target; the second fraction defines the volume of healthy tissue receiving a dose greater than or equal to the prescribed reference dose. The CI ranges from 0 to 1, where 1 is the ideal value. A value close to 0 indicates either total absence of conformation, i.e., the target volume is not irradiated or there is a very large volume of irradiation compared to the target volume.[93]

Dose homogeneity characterizes the uniformity of dose distribution within the target volume. The homogeneity index is defined as:

$$HI = (D_{2\%} - D_{98\%})/D_{50\%}$$

(eq. 5)

where the $D_{2\%}$ is the near maximum dose, the $D_{98\%}$ is the near minimum dose and the $D_{50\ \%}$ is the median dose suggested as the normalization value by ICRU 83.[94] An HI of zero indicates that the dose distribution is almost homogeneous.

4.10 Planning verification

For QA purposes, the initial plans made for each patient and for each technique with and without FF were recalculated on a CT scan of the phantom. The plans were recalculated on the artificial CT scan of the Delta4 keeping all other parameters identical to the patient plan, and placing the isocenter in the center of the cylindrical

Delta4 phantom geometry. Dose distributions have been calculated using the Monte Carlo algorithm with 1% Monte Carlo variance. The calculation grid was 2mm.

The DICOM RT objects, such as RT Dose (calculated in the phantom), RT Dose per beam and RT plan (beam arrangements) were exported to the *ScandiDos* software (Scandidos, Uppsala, Sweden).

First, the output of the accelerator was measured using an ionization chamber and the Delta4 daily output correction factor was set to compensate for any deviation from calibration conditions.

The Delta4 and associated devices were positioned and aligned in the Linac couch. The DICOM RT objects were imported in the *ScandiDos* software. The IMRT and the VMAT plans with FF were then delivered to the Delta4 phantom. Without changing any setup, the hard drive of the LCS was changed to allow for the delivery of FFF beams. The IMRT and the VMAT plans without FF were then delivered to the Delta4 phantom.

In measurement mode, raw readings were converted to dose by applying a number of correction factors. The response of the dosimetry equipment was compared with the calculated dose matrices by gamma evaluation.

4.11 Gamma Index

The quantitative comparison of two-dimensional dose distributions, e.g. calculated versus measured has become a key issue in multi-dimensional dosimetry with the implementation of IMRT.[51]

In 1998 Low *et al.*[95] proposed the γ evaluation method for the quantitative evaluation of two-dimensional dose distributions. This concept combines a dose difference criterion with a distance-to-agreement (DTA) criterion for each point of interest. The DTA specifies the distance from one measured point to the closest calculated point of the same dose. The criterion is used because of the fact that a spatial difference in a high gradient area can correspond to a large dose difference.

The γ index evaluation method has the advantage of being able to determine calculation accuracy for plans with a complex gradient composition, e.g. IMRT and VMAT plans, as it simultaneously takes into account both dose differences and DTA without distinguishing between areas of different gradient size.[96]

For the present work, the criteria of a combination of three parameters proposed by Stock *et al*.[15] given in Table 4.4 were used. Based on the results of their work with 10 IMRT hybrid plans verified with film and polystyrene phantom, they developed a decision filter looking at γ_{mean} values, the average number of pixels with $\gamma>1$, and the maximum γ value expressed as the 1st percentile ($\gamma_{1\%}$).

Such a type of recommendation depends on the chosen set of gamma evaluation criteria, in this case a dose difference, relative to dose maximum, of 3% and 3mm DTA criteria was used, the same that is applied clinically at the Medical University of Vienna. The same criteria were used in the γ evaluation for both flattened and unflattened treatment plans.

Table 4.4 Criteria for acceptability of gamma evaluations of pre-treatment verification of IMRT beams.[15]

Approach	Average gamma	Maximum gamma	$\gamma_{\%}> 1$
Acceptable	< 0.5	< 1.5	0 – 5%
Need further evaluation	0.5 – 0.6	1.5 – 2.0	5 – 10%
Not acceptable	> 0.6	> 2.0	> 10%

5 Results and Discussion

In this chapter, a summary of the major results is presented and discussed.

5.1 Clinical Acceptable Plans

For each patient a set of clinically acceptable plans with similar DVHs was created for all modalities, as shown in figure 5.1.

IMRT plans and VMAT plans as similar OAR DVHs and similar PTV DVHs achieved during treatment planning. The PTV as the same median dose, which is a prerequisite to achieve similar and thus comparable clinical conditions with respect to tumor control.

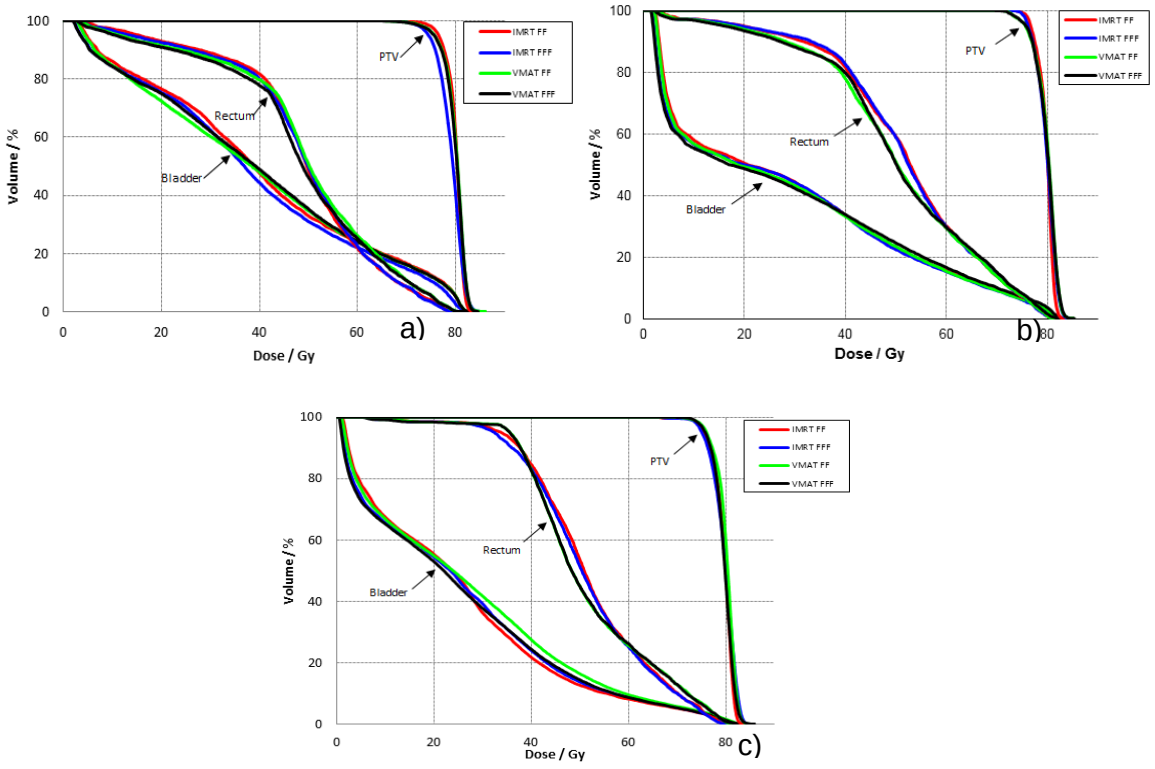

Figure 5.1. Initial DVHs generated for the three prostate cases, for IMRT using FF (red) and FFF beams (blue) and for VMAT using FF (green) and FFF beams (black).

During inverse planning, sequencing is performed by the TPS and the sequencer was able to deal with unflattened beams. In order to achieve comparable IMRT treatment plans the segment shapes and number of segments were different for IMRT plans with flattened and unflattened beams; this will be discussed later on.

For the three prostate cases, results of the dose metrics according with ICRU 83 are summarized in Table 5.1. The $D_{near\text{-}min}=D_{98\%}$, $D_{near\text{-}max}=D_{2\%}$ and $D_{50\%}$ (median) are indicated for the PTV. The $V_{95\%}$ is the volume (%) that receives at least 95% of the prescribed dose is also reported in Table 5.1.

Table 5.1 The dose-volume metrics presented as mean values ± 1SD

	Patient 1			
	IMRT FF	**IMRT FFF**	**VMAT FF**	**VMAT FFF**
$D_{98\%}$(PTV) Gy	74.3 ± 1.2	74.1 ± 0.9	72.6 ± 1.0	72.7 ± 0.9
$D_{2\%}$(PTV) Gy	82.1 ± 0.1	82.9 ± 0.1	83.1 ± 0.1	83.2 ± 0.1
$D_{50\%}$(PTV) Gy	79.7 ± 0.2	79.9 ± 0.2	79.8 ± 0.5	79.9 ± 0.3
$V_{95\%}$(PTV) %	97.8 ± 2.2	97.9 ± 1.5	95.1 ± 2.5	95.6 ± 1.9
	Patient 2			
	IMRT FF	**IMRT FFF**	**VMAT FF**	**VMAT FFF**
$D_{98\%}$(PTV) Gy	73.2 ± 1.4	72.3 ± 1.1	72.3 ± 1.0	72.3 ± 0.8
$D_{2\%}$(PTV) Gy	82.4 ± 0.0	83.3 ± 0.0	83.1 ± 0.1	83.0 ± 0.0
$D_{50\%}$(PTV) Gy	79.9 ± 0.4	79.6 ± 0.4	79.9 ± 0.5	79.9 ± 0.4
$V_{95\%}$(PTV) %	96.4 ± 2.3	94.6 ± 2.5	95.3 ± 2.1	95.3 ± 2.0
	Patient 3			
	IMRT FF	**IMRT FFF**	**VMAT FF**	**VMAT FFF**
$D_{98\%}$(PTV) Gy	72.1 ± 1.6	71.9 ± 1.5	72.9 ± 1.4	72.8 ± 1.2
$D_{2\%}$(PTV) Gy	82.4± 0.1	83.5 ± 0.1	83.2 ± 0.1	83.1 ± 0.0
$D_{50\%}$(PTV) Gy	79.6 ± 0.4	79.8 ± 0.3	79.8 ± 0.3	79.4 ± 0.4
$V_{95\%}$(PTV) %	95.1 ± 2.2	94.4 ± 2.4	96.1 ± 2.2	95.4 ± 2.5

The use of multiple dose-volume constraints (e.g., D_{median}, $D_{98\%}$, $D_{95\%}$, $D_{2\%}$) for each defined volume leads to more precision in the planning aims and is therefore recommended by ICRU 83.

For the first patient the VMAT plans, on average, delivered slightly a higher dose to the PTV than did the IMRT plans, this is characterized by a higher near maximum dose $D_{2\%}$. For the second and third patient the IMRT FFF, deliver slightly a higher dose, compared to the other techniques.

However no major differences were observed between the techniques. For the target volume, the unflattened beams offered comparable dosimetric coverage as compared to flattened beams.

5.1.1 Dose Distributions

Figure 5.2 shows CT images with isodose lines for the first prostate patient. All the beams in figure 5.2 are 10 MV photons. For each patient, plans have been produced for IMRT and VMAT with and without FF. The image a) and b) show IMRT plans with flattened and unflattened beams, respectively; while c) and d) show VMAT plans with flattened and unflattened beams, respectively.

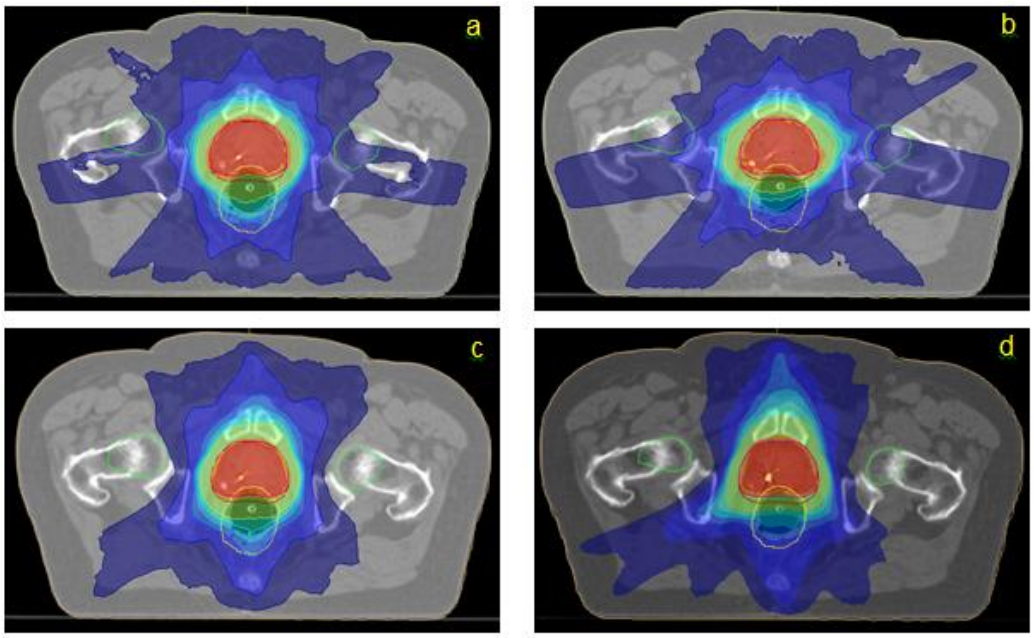

Figure 5.2. Planning CT images with isodose lines for the first prostate patient. Images a and b show IMRT plans with flattened and unflattened beams, respectively; while c and d show VMAT plans with flattened and unflattened beams, respectively. Isodose lines represent planned doses of 78 Gy (red), 55 Gy (green), 30 Gy (blue) and 20 Gy (dark blue).

Apparently, the plans developed with flattened and unflattened beams look very similar, for this patient. However, there is a slightly difference, in the volume of the the 20 Gy isodose line (dark blue) that seems to be higher for IMRT plans, the isodose line tends to be slightly closer to the surface in IMRT plans (a and b) than in VMAT plans (c and d).

Figure 5.3 shows the comparison of dose distributions for the three prostate patients. For each patient VMAT plans are shown: with flattened and unflattened beams.

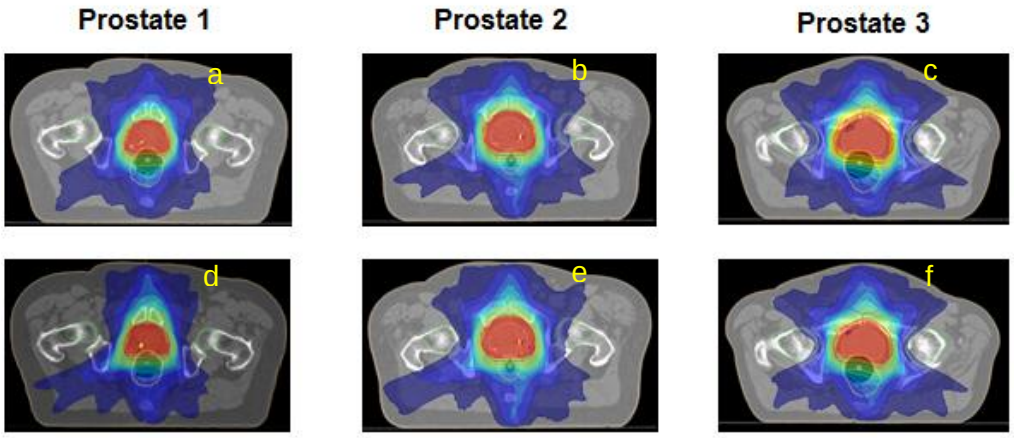

Figure 5.3. Planning CT images with isodose lines for three patients. Images a, b and c show VMAT plans with flattened 10MV beams while d, e and f show plans with unflattened beams. Isodose lines represent planned doses of 78 Gy (red), 55 Gy (green), 30 Gy (blue) and 20 Gy (dark blue).

5.2 Pareto Fronts

Pareto fronts were successfully sampled for all cases. As in the study of Ottosson *et al.*[31] the results demonstrate that the sampled Pareto fronts follow the definition of the Pareto concept, i.e. no solution simultaneously improving, or deteriorating, both parameters was found.

Plans belonging to the same technique (IMRT FF, IMRT FFF, VMAT FF, VMAT FFF) constitute the pareto front, enabling comparison of techniques rather than plan to plan.

The Pareto fronts generated with the four different techniques for case 1 are plotted in the same diagram, Figure 5.4.

The solid line in figure 5.4 is marking the 5% loss of target coverage.

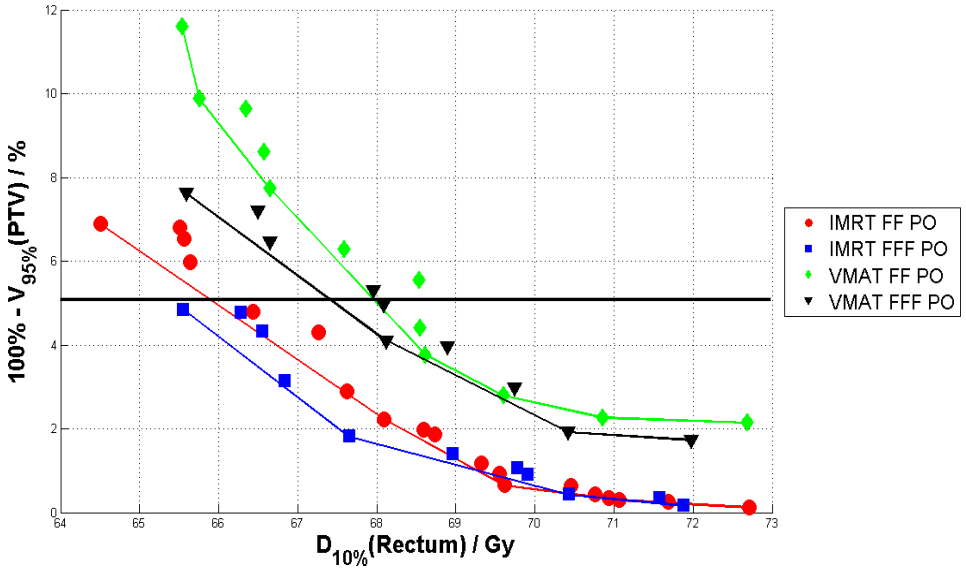

Figure 5.4. Pareto optimal fronts for the first prostate case (191 plans), for IMRT with FF (red circles), IMRT without FF (blue squares), VMAT with FF (green diamonds) and VMAT without FF (black triangles).

The IMRT FFF front is situated below and to the left of the other fronts indicating that this technique exhibit a better combination of target coverage and less dose to the rectum, compared to the others.

The IMRT fronts starts with almost the same target coverage, but the loss of coverage is slightly faster for the IMRT FF. The same happens for the VMAT fronts, however starting with higher under dosage. Comparing these two fronts the decrease in coverage of the VMAT FF front is much faster than the VMAT FFF front.

For the IMRT fronts the $D_{10\%}$ of the rectum is about 66Gy for the 5% loss of target coverage while for the VMAT fronts for the same loss of target coverage the $D_{10\%}$ is about 1.5Gy higher.

Note that the x axis in figure 5.4 goes up to 12%.

After the import of the DVHs in MATLAB and plot all the results from the dose distributions of the plans from the first patient, it was noticed that most of them are non pareto optimal plans. The fronts were created with less number of plans, and no major differences have been observed in the fronts, as shown in figure 5.5. The minor difference is that IMRT FFF front reaches the 5% loss of target coverage slightly before the IMRT FF front.

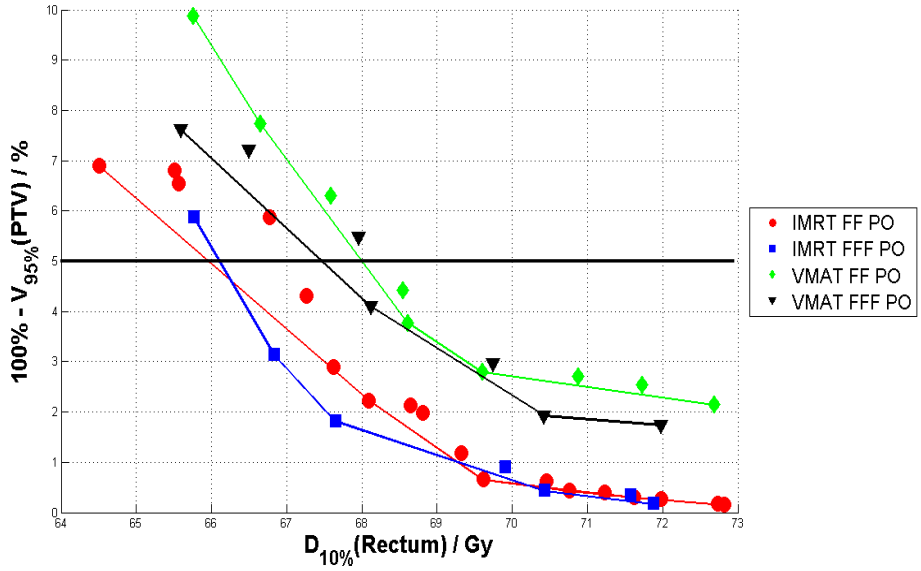

Figure 5.5. Pareto optimal fronts generated for the first prostate case (88 plans), for IMRT with FF (red circles), IMRT without FF (blue squares), VMAT with FF (green diamonds) and VMAT without FF (black triangles).

The Pareto fronts generated with the four different techniques for case 2 are plotted in figure 5.6.

For this case the IMRT FF front was situated below and to the left of the other fronts indicating that this technique is better compared to the others.

In this case the IMRT FFF front starts with higher under dosage than IMRT FF, but is situated below the VMAT fronts. At 5% loss of target coverage the IMRT optimal fronts, differed by about 1 Gy, in favour for IMRT FF.

Regarding the VMAT technique, virtually no difference was observed between the Pareto optimal fronts of VMAT and VMAT FFF. While comparing the IMRT FF front with the VMAT fronts at 5% loss of target coverage the difference is about 2.5 Gy, as shown in figure 5.6.

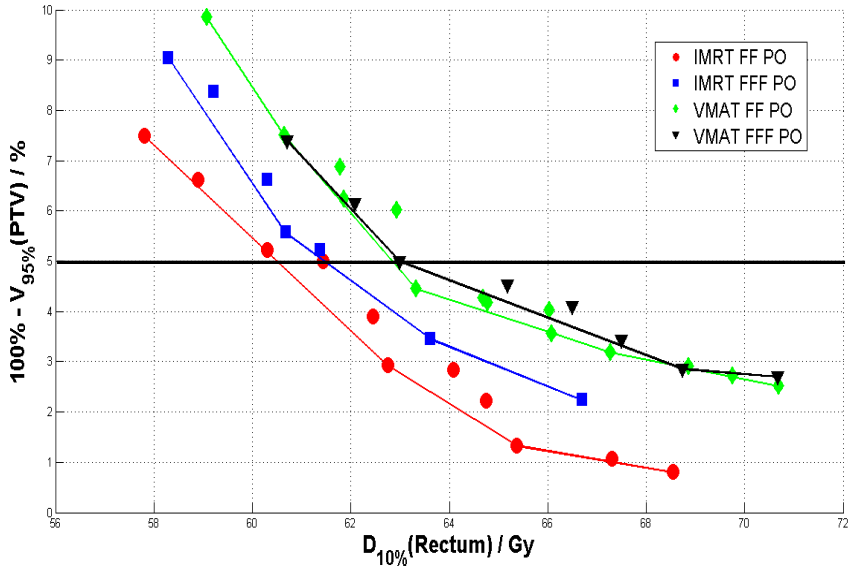

Figure 5.6. Pareto optimal fronts generated for the second prostate case (76 plans), for IMRT with FF (red circles), IMRT without FF (blue squares), VMAT with FF (green diamonds) and VMAT without FF (black triangles).

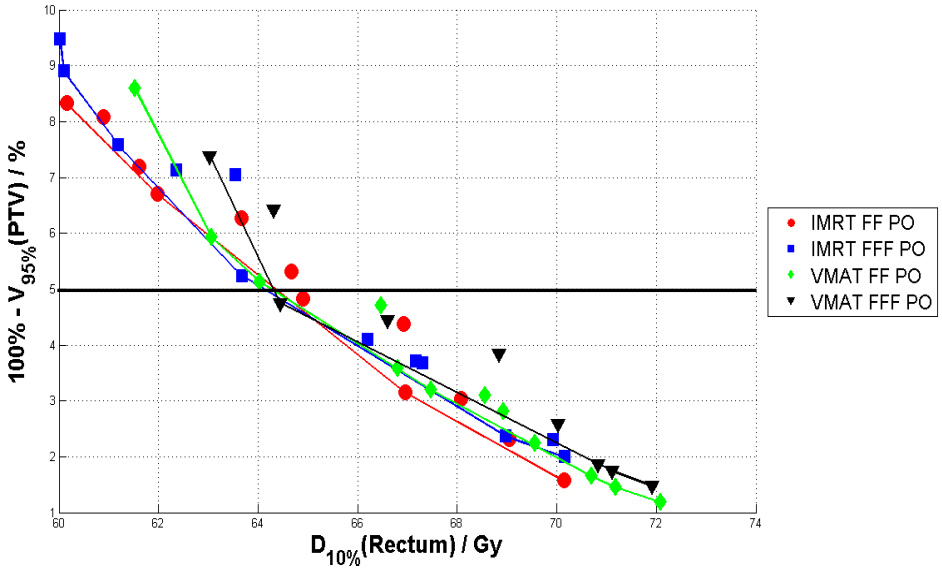

Figure 5.7. Pareto optimal fronts generated for the third prostate case (75 plans), for IMRT with FF (red circles), IMRT without FF (blue squares), VMAT with FF (green diamonds) and VMAT without FF (black triangles).

For the third case, the fronts laid virtually on top of each other, even if the IMRT FF front starts with better target coverage, the difference between the fronts is insignificant.

By not changing any cost function parameter, except for the rectum used for the fronts, and by rejecting plans where the doses to the PTV were compromised, the dose to these OAR were consistent for all the techniques and all plans generated, as shown in figure 5.7

5.2.1 Plan comparison

From the analyses of the Pareto optimal fronts, can be observed that PTV coverage is deteriorated with the decrease of the $D_{10\%}$ of the rectum.

For the first and the second cases, IMRT plans appears to be favorable compared with the VMAT plans, while for the third case, no significant difference was observed. All the techniques performed considerably better for case 2 compared to case 1 and 3.

All the plans generated had to be sorted to present a Pareto front. This required a large number of plans made by varying the EUD maximum for the rectum in smaller steps.

For the first patient with 191 plans, a huge number of non Pareto optimal plans were generated. This could be a result of the way the TPS works. In the first stage the optimized fluence maps are created and the dose distribution is calculated with a finite size pencil beam algorithm. The optimizer stops automatically when it could not improve one objective without deteriorating at least one of the others, i. e., when the system found a Pareto optimal plan. But in the second stage, the sequencer tries to rebuild these fluence maps by optimizing the number and shape of the segments for each beam, and may not always reach a Pareto optimal plan. Decreasing the Monte Carlo variance, i. e., increasing the number of histories, may help the system to find a better solution but this could increase the planning time and the plans can become more complex and difficult to be delivered.

5.3 Treatment time, MU requirements and Segments

- **Treatment time**

The treatment time to deliver a single fraction was measured from the start of the first beam to the end of the last beam, for IMRT plans; and from the start of the 360º arc to the end.

Table 5.2 The average time (min), to deliver the initial plans produced for each patient, the average of monitor units per fraction required for the same prescription, and the average of the total number of segments (seg) of flattened/unflattened for the different techniques

	T [min:sec]		MU		Seg	
	IMRT	VMAT	IMRT	VMAT	IMRT	VMAT
Prostate 1	07:49/ 06:15	02:29/ 03:10	283.2/ 321.4	395.2/ 434.5	57/ 58	96/ 96
Prostate 2	07:16/ 05:58	03:14/ 03:58	308.7/ 362.4	483.1/ 546.6	55/ 48	108/ 108
Prostate 3	07:34/ 06:05	02:43/ 03:19	291.4/ 324.7	451.2/ 496.1	53 /51	108 /108

For the first patient, the measured treatment time of the initial plans was about 8 minutes for IMRT FF. By the use of IMRT FFF the treatment time was reduced by 25% for IMRT FFF (about 6 minutes) and decreased even further for both VMAT techniques.

For the second case the decrease in the treatment time is similar. The measured time of the initial plans was about 7.25 minutes for IMRT FF, and without FFF the treatment time was reduced by 22%, decreasing even further for VMAT.

For the third patient the decrease in the treatment time was about 24% between the IMRT FF and the IMRT FFF. As for the other cases the VMAT treatment time was even lower.

Comparing the two techniques, IMRT and VMAT with unflattened beams, the decrease in the treatment time is about 1.8 times lower in favor for VMAT.

For the VMAT plans the treatment time increased by a factor of 28%, 23% and 22%, for case 1, case 2 and case 3, respectively. This fact was may be due to the huge increase in the number of monitor units for the VMAT FFF plans.

- **Monitor Units**

The average of MUs for the prostate cases treatment plans, both for IMRT and VMAT, with and without flattening filter are listed in table 5.2.

For the three prostate cases, the lowest numbers of MUs were observed for IMRT FF with a mean value of 283, 309 and 291 MUs, respectively. For VMAT FFF the highest numbers of MUs were observed for the case 2 with a mean value of 547 MUs. In general the number of MUs was always higher for the VMAT FFF technique.

Although, the number of MU tends to be higher for IMRT FFF, VMAT FF and VMAT FFF, the use of these techniques lead to an increase of time efficiency compared to IMRT FF.

The results presented are consistent with Wang *et al*[97]*.* that recently reported that the number of MUs for FFF mode could be 10-16% higher for prostate cases. In this case the increase of the MUs for the IMRT FFF plans was about 13%, 15% and 10% for case 1, 2 and 3, respectively. Regarding the VMAT plans the increase for the three prostate cases were about 9%, 12% and 9%, respectively.

This is an expected consequence of unflattened delivery because of the shape of the beam profile; delivering any dose off-axis will require the beam to be on for a longer period of time.

- **Segments**

Table 5.2 compares the number of segments required to deliver the same dose distribution with two techniques: IMRT with FF and FFF and VMAT with and without FF. Taking the ratio of (unflattened IMRT/conventional IMRT) for each of the three prostate cases, the average for the number of segments required was 1.02, 0.87 and 0.96, for case 1, case 2 and case 3, respectively. For the VMAT plans no difference in the average number of segments was noticed.

In most cases, the number of segments needed for an unflattened beam is slightly more than that for the corresponding flattened beam. In this case this assumption was not verified.

5.4 CI and HI

The values of CI and HI for the three prostate treatment plans were computed and tabulated in table 5.3.

In general the conformation was better for the VMAT plans and was worse for the IMRT FF.

To quantify dose uniformity in the PTV, it was calculated for each plan the homogeneity index. An HI of zero indicates that the dose distribution is almost homogeneous.

For the three cases, no significant differences were found between treatment plans with flattened and those using unflattened beams. Nevertheless better homogeneity indices were found for the IMRT FF plans with better homogeneous dose distribution.

Table 5.3 Comparison of the CI and HI in the IMRT and VMAT plans with and without FF for the three prostate cases

	Conformity Index			
	IMRT FF	**IMRT FFF**	**VMAT FF**	**VMAT FFF**
Prostate 1	0.81 ± 0.02	0.81 ± 0.02	0.83 ± 0.01	0.82 ± 0.02
Prostate 2	0.86 ± 0.01	0.86 ± 0.01	0.88 ± 0.01	0.86 ± 0.01
Prostate 3	0.85 ± 0.02	0.86 ± 0.02	0.88 ± 0.01	0.88 ± 0.01
	Homogeneity Index			
	IMRT FF	**IMRT FFF**	**VMAT FF**	**VMAT FFF**
Prostate 1	0.10 ± 0.02	0.11 ± 0.01	0.13 ± 0.01	0.13 ± 0.01
Prostate 2	0.12 ± 0.02	0.14 ± 0.02	0.14 ± 0.01	0.14 ± 0.01
Prostate 3	0.13 ± 0.02	0.15 ± 0.02	0.13 ± 0.02	0.13 ± 0.02

5.5 Gamma evaluation

The agreement between the measurements, performed with the Delta 4 phantom, and calculations made in Monaco^{TM} were compared for the three prostate cases, for the four initial plans of each technique. The results of the gamma evaluation are listed in table 5.4.

Table 5.4 Gamma index evaluation: results of the comparison between measured (Delta4) and calculated (Monaco^{TM})

	γ-mean				**γ-max**				**$\gamma \leq 1$ (%)**			
	IMRT FF	**IMRT FFF**	**VMAT FF**	**VMAT FFF**	**IMRT FF**	**IMRT FFF**	**VMAT FF**	**VMAT FFF**	**IMRT FF**	**IMRT FFF**	**VMAT FF**	**VMAT FFF**
Patient 1	0.21	0.22	0.22	0.43	1.21	1.08	0.98	1.82	99.6	99.6	100	90.2
Patient 2	0.25	0.28	0.22	0.32	1.04	1.65	0.89	1.20	99.8	97.7	100	99.1
Patient 3	0.23	0.30	0.24	0.33	0.96	1.50	0.90	1.45	100	97.2	100	95.9

The gamma value averaged over all measured pixels was calculated. This value gives information about how close the calculation is to the measurement averaged over the

area of measurement. The lower the value the better the agreement. The average number of pixels with γ≤1, and the maximum γ value expressed as the 1st percentile ($\gamma_{1\%}$) was also calculated.

For the three patients the four initial plans were measured with the Delta 4 phantom and analyzed with *Scandidos* software. The gamma analyzes was performed.

Averaged over these 3 patients, four planes per patient, one per each technique, the mean gamma values for IMRT FF, IMRT FFF, VMAT FF and VMAT FFF, were 0.23, 0.27, 0.23 and 0.36, respectively. These results showed high agreement with calculated values. For the same plans, the percentage of plans with a gamma smaller than 1 was 99.8%, 98.2%, 100% and 95.1%, respectively.

For the prostate 1, the γ-mean for VMAT FF plan was 0.43, filling the acceptability criteria, but in average the number of pixels exceeding a gamma of 1.0 was 9.78%. This is an acceptable value; however other verification tools such as angle distribution, dose difference map, profiles are needed for further evaluation. A more detailed investigation concerning the dose calculation accuracy is beyond the scope of this study and will be studied later on.

In general techniques with flattened beams showed a better agreement between measurements and calculations.

Due to the non-uniform shape of the flattening filter, the beam energy distribution will vary with the off-axis distance. In theory the removal of the flattening filter facilitates the dose calculation and might improve the dose calculation accuracy of advanced algorithms.[17] However this was not observed in this study.

6 Conclusions and Future work

This study contributed to a professional enrichment in the treatment planning field and will help in the implementation of flattening filter free Linacs at the Portuguese Radiotherapy departments.

When a new technique is being introduced, in this case a flattening filter free beam from a conventional accelerator, it is needed to explore the properties and the potential benefits and drawbacks of using unflattened beams.

The dosimetric properties of the unflattened beams were studied and the feasibility of developing clinically acceptable treatment plans using unflattened beams, and compare them with typical plans developed with flattened beams was the aim of this study.

The results show that it was possible to develop clinically acceptable plans for IMRT and VMAT, with flattened and unflattened beams. In terms of dose distribution, treatment plans with flattened and unflattened beams were of similar plan quality. The same median dose was achieved for all modalities, which is a prerequisite to achieve similar and comparable clinical conditions with respect to tumor control.

Due to different planning philosophies and/or poor statistics, conventional planning studies based on DVHs comparison often lead to inconclusive results. It is believed that the use of Pareto optimal fronts will reduce these influences. Therefore the feasibility of Pareto optimal fronts to compare the two delivery techniques has been evaluated.

The results indicate that the use of Pareto fronts is a feasible approach to compare different techniques and technologies for advanced radiotherapy.

Comparing Pareto fronts instead of single plans gives a clearer view of the whole picture. The whole range of doses to an OAR can be assessed at the same time and correlated with the target coverage. If two single plans are compared the position on the Pareto front could be missed or the selected plan might not be Pareto optimal.

The Pareto optimal fronts give also information that is not accessible in a DVH. This can be seen, for the first and the third patient. For the first patient the IMRT fronts show

that is possible to spare the rectum without losing target coverage, the same happens in the second case for the VMAT techniques.

For the cases studied the IMRT fronts were generally found to be more favorable. Nevertheless one should not set aside the possibility of using VMAT plans, as there might be cases benefiting from this technique, as already reported in several papers.[55,97-100]

In order to perform the Pareto fronts to compare the four techniques, equivalent treatment plans were performed. To be equivalent to a full arc VMAT plan, an IMRT plan with nine beams have been created, however this is not the number of beams used in clinical routine. This amount of beams give more degrees of freedom to the system and let the system create a more conformal dose distribution; however the treatment time increased largely and the low doses must be evaluated.

Another application for the Pareto fronts is to use them to aid treatment planning. It would be advantageous if patients could be selected prior to treatment planning, based on some criteria. The selection criteria could include patient size and tumor location, tumor size and proximity to other structures, etc. However, this is beyond the scope of this work and could be a subject of future investigations.

This study shows that for IMRT without flattening filter, the treatment delivery time reduces by about 24%, and even further for VMAT techniques with and without FF.

However, total MUs are much larger for FFF delivery for all the cases due to the non-flatness of the dose profile. Accordingly with Wang *et al.* the number of MUs for unflattened beams could be 10-16% higher for prostate cases. This study reports an increase in the number of monitor units of 9-15% for unflattened beams compared to conventional IMRT and VMAT beams. With different optimization algorithms and segmentation algorithms, adjusted for unflattened beams the number of monitor units of the unflattened/flattened IMRT/VMAT plans may reduce, and consequently the treatment delivery times may reduce even further.

The TPS Monaco^{TM} has been commissioned for unflattened beams. The initial treatment plans performed for each patient and for each technique were measured and compared with calculations, by gamma analyses. The results of the mean gamma value, the average number of pixels with $\gamma \leq 1$, and the maximum γ value expressed as the 1st percentile ($\gamma_{1\%}$) showed a very good agreement between measurements and calculations.

In theory, the dosimetric characteristic of unflattened beams facilitates dose calculation and might improve the dose calculation accuracy of advanced algorithms. The calculation accuracy of the unflattened beams was beyond the scope of this study and will be subject of future investigations.

6.1 Study limitations

This study has been performed with a non-clinical version of Monaco^{TM}. The TPS sequencer was able to deal with unflattened beams and to create plans with similar plan quality comparing with conventional IMRT and VMAT plans. Nevertheless it was noticed that some improvements should be done in the optimization and segmentation algorithms, in order to give better results for unflattened beams.

7 References

1. Boge J, inventor; Gundersen Clinic, Ltd. La Crosse, Wis, assignee. External X-Ray Beam Flattening Filter. United States patent US 3,917,954. 1975 Nov 4.
2. Kry SF, Titt U, Pönisch F, Vassiliev ON, Salehpour M, Gillin M, et al. Reduced neutron production through use of a flattening- filter-free accelerator. Int J Radiat Oncol Biol Phys 2007; 68(4):1260–4.
3. Vassiliev ON, Kry SF, Kuban DA, Salehpour M, Mohan R, Titt U. Treatment planning study of prostate cancer intensity-modulated radiotherapy with a Varian Clinac operated without a flattening filter. Int J Radiat Oncol Biol Phys 2007; 68:1567–71.
4. Cashmore J. The characterization of unflattened photon beams from a 6 MV linear accelerator. Phys Med Biol 2008; 53:1933–46.
5. Mesbahi A, Nejad FS. Monte Carlo study on a flattening filter-free 18-MV photon beam of a medical linear accelerator. Radiat Med 2008;26(6):331–6.
6. Vassiliev ON, Kry SF, Chang JY, Balter PA, Titt U, Mohan R. Stereotactic radiotherapy for lung cancer using a flattening filter free Clinac. Journal of applied clinical medical physics/American College of Medical Physics 2009;10(1):2880.
7. Wiezorek T, Georg D, Schwedas M, Salz H, Wendt TG. Experimental determination of peripheral photon dose components for different IMRT techniques and linear accelerators. Z. Med.Phys. 2009; 19:120–128.
8. Stathakis S, Esquivel C, Gutierrez A, Buckey CR, Papanikolaou N. Treatment planning and delivery of IMRT using 6 and 18MV photon beams without flattening filter. Appl Radiat Isot 2009; 67:1629–37.
9. Kragl G, Baier F, Lutz S, Albrich D, Dalaryd M, Kroupa B, Wiezorek T, Knöös T, Georg D. Flattening filter free beams in SBRT and IMRT: dosimetric assessment of peripheral doses. Z Med Phys 2010, article in press.
10. Fu W, Dai J, Hu Y, Han D, Song Y. Delivery time comparison for intensity modulated radiation therapy with/without flattening filter: a planning study. Phys Med Biol 2004; 49:1535–47.

11. Kragl G, af Wetterstedt S, Knausl B, Lind M, McCavana P, Knöös T, *et al*. Dosimetric characteristics of 6 and 10MV unflattened photon beams. Radiother Oncol 2009; 93(1):141–6.

12. Kragl G, Baier F, Lutz S, Albrich D, Dalaryd M, Kroupa B, Wiezorek T, Knöös T, Georg D. Flattening filter free beams in SBRT and IMRT: dosimetric assessment of peripheral doses. Z Med Phys 2010, article in press.

13. Georg D, Kragl G, af Wetterstedt S, McCavana P, McClean B, Knöös T. Photon beam quality variations of a flattening filter free linear accelerator. Med Phys 2010; 37(1):49–53.

14. Kim T, Zhu L, Suh T, Geneser S, Xing L, Meng B. Inverse planning for IMRT with nonuniform beam profiles using total-variation regularization (TVR). Journal of Applied Clinical Medical Physics 2011; 38(1):57-66.

15. Stock M, Kroupa B, Georg D. Interpretation and evaluation of the gamma index and the gamma index angle for the verification of IMRT hybrid plans. Phys. Med. Biol. 2005; 50: 399-411.

16. Bentel GC. Radiation therapy planning. 2nd ed. USA: McGraw-Hill Companies; 1996. ISBN-007005115-1

17. Georg D, McClean B, Knöös T. Current status and future perspective of flattening filter free photon beams. Med Phys 2011; 38:1280-94.

18. ICRU Report 33: Radiation quantities and Units. Washington, DC; 1980.

19. Martin JE. Physics for Radiation Protection: A Handbook. 2nd ed. USA: WILEY-VCH; 2006. 822p.

20. Shapiro J. Radiation Protection - A guide for Scientists, Regulators and Physicians. 1st ed. Harvard University Press. USA: La Editorial; 2002. 663p.

21. Zhu T, Ahnesjö A, *Leung* K, Lam KL, Li X, Sharpe M *et al.* Report of AAPM Therapy Physics Committee Task Group 74: In-air output ratio for megavoltage photon beams. Med. Phys. 2009; 36:5262-9.

22. Galvin J, Ezzel G, Eisbruch A, *et al.* Implementing IMRT in clinical practice: a joint document of the American Society for Therapeutic Radiology and Oncology and the American Association of Physicists in Medicine. Int J Radiat Oncol Biol Phys. 2004; 58(5):1616–34.

23. Otto K. Volumetric modulated arc therapy: IMRT in a single gantry arc. Med Phys. 2008; 35(1): 310.

24. Briesmeister JF. MCNP—a general Monte Carlo N-particle transport code, version 4C. Report LA-13709-M. Los Alamos, NM: Los Alamos National Laboratory; 2000.

25. Metropolis N. The beginning of the MC Method. Los Alamos Sci. 1987; 15:125–130.

26. Bielajew AF. Fundamentals of the Monte Carlo method for neutral and charged particle transport. The University of Michigan, 2001.

27. Sidek M. Monte Carlo investigations of radiotherapy beams: studies of conventional, stereotactic and unflattened beams. [Doctor's thesis]. [Birmingham (UK)]: University of Birmingham; 2010. 243 p.

28. Niemierko A. Reporting and analyzing dose distributions: A concept of equivalent uniform dose. Med Phys 1997; 24:103–110.

29. Pareto V. Cours d'Economie Politique. Paris: F. Pichou; 1897.

30. Juran JM. Quality control handbook. 3rd ed. New York: McGraw-Hill; 1974.

31. Ottosson R, Engstroom PE, Sjoostroom D, Behrens C, Karlsson A, Knoos T, Ceberg C. The feasibility of using pareto fronts for comparison of treatment planning systems and delivery techniques. Acta Oncologica. 2009; 48(2):233-237.

32. Becker J. Simulation of neutron production at medical linear accelerator. [Diploma thesis]. [Hamburg (Germany)]: Institute of Experimental Physics University of Hamburg; 2007. 138 p.

33. Bentel GC. Radiation therapy planning. 2nd ed. USA: McGraw-Hill Companies; 1996. ISBN-007005115-1

34. Metcalfe P, Kron T, Hoban P. The Physics of Radiotherapy X-rays from Linear Accelerators. 3rd ed. Wisconsin: Medical Physics Publishing; 2004. 493p. ISBN-0-944838-75-6

35. Lind M. Characteristics of a Flattening Filter Free Photon Beam – Measurements and Monte Carlo Simulations [master's thesis]. [Lund (Sweden)]: Lund University; 2008. 55 p.

36. Metcalfe P, Kron T, Hoban P. The Physics of Radiotherapy X-rays from Linear Accelerators. 3rd ed. Wisconsin: Medical Physics Publishing; 2004. 493p. ISBN-0-944838-75-6

37. Webb S. The physical basis of IMRT and inverse planning. The British Journal of Radiology 2003; 76: 678–689.

38. Pönisch F, Titt, U, Vassiliev, ON, Kry, SF and Mohan, R. Properties of unflattened photon beams shaped by a multileaf collimator. Med Phys 2006; 33(6), 1738-1746.

39. Vassiliev ON, Titt U, Ponisch F, Kry SF, Mohan R, Gillin MT. Dosimetric properties of photon beams from a flattening filter free clinical accelerator. Phys Med Biol 2006; 51:1907–1917.

40. Pearson D, Parsai E and Feldmeier J, Evaluation of dosimetric properties of 6 & 10 MV photon beams from a Linear accelerator with no flattening filter. Med Phys 2006; 33(6):2099.

41. Titt, U, Vassiliev, ON, Pönisch, F, Kry, SF and Mohan, R. Monte Carlo study of backscatter in a flattening filter free clinical accelerator. Med Phys 2006; 33(9), 3270-3273.

42. Zhu XR, Kang Y, Gillin MT. Measurements of in-air output ratios for a linear accelerator with and without the flattening filter. Med. Phys. 2006; 33:3723–3733.

43. Mesbahi A, Mehnati P, Keshtkar A, Farajollahi A. Dosimetric properties of a flattening filter-free 6-MV photon beam: a Monte Carlo study. Radiat Med 2007; 25:315–24.

44. Mesbahi A. Dosimetric characteristics of unflattened 6MV photon beams of a clinical linear accelerator: a Monte Carlo study. Appl Radiat Isot 2007; 65:1029–36.

45. Kragl G, af Wetterstedt S, Knausl B, Lind M, McCavana P, Knöös T, et al. Dosimetric characteristics of 6 and 10MV unflattened photon beams. Radiother Oncol 2009;93(1):141–6.

46. Georg D, Kragl G, af Wetterstedt S, McCavana P, McClean B, Knöös T. Photon beam quality variations of a flattening filter free linear accelerator. Med Phys 2010; 37(1):49–53.

47. Kragl G. New technological approaches to advanced radiation therapy: Flattening filter free photon beams [dissertation]. [Vienna (Austria)]: Medical University of Vienna; 2010. 94 p.

48. Dalaryd M, Kragl G, Ceberg C, Georg D, McClean B, Af Wetterstedt S, Wieslander E, Knöös T A Monte Carlo study of a flattening filter-free linear accelerator verified with measurements. Phys. Med. Biol. 2010; 55:7333–7344.

49. Kry SF, Howell RM, Titt U, Salehpour M, Mohan R, Vassiliev ON. Energy spectra, sources, and shielding considerations for neutrons generated by a flattening filter free Clinac. Med Phys. 2008; 35(5):1906-11.

50. Kry SF, Howell RM, Polf J, Mohan R, Vassiliev ON. Treatment vault shielding for a flattening filter-free medical linear accelerator. Phys Med Biol 2009; 54(5):1265–73.

51. Intensity Modulated Radiation Therapy Collaborative Working Group. Intensity-modulated radiotherapy: current status and issues of interest. Int J Radiat Oncol Biol Phys 2001; 51(4):880-914.

52. Kim T, Zhu L, Suh T, Geneser S, Xing L, Meng B. Inverse planning for IMRT with nonuniform beam profiles using total-variation regularization (TVR). Journal of Applied Clinical Medical Physics 2011; 38(1):57-66.

53. Rao M, Yang W, Chen F, Sheng K, Ye J, Mehta V, Shepard D, Cao D. Comparison of Elekta VMAT with helical tomotherapy and fixed field IMRT: Plan quality, delivery efficiency and accuracy. Med. Phys. 2010; 37:1350–1359.

54. Guckenberger M, Richter A, Krieger T, Wilbert J, Baier K, Flentje M. Is a single arc sufficient in volumetric-modulated arc therapy (VMAT) for complex-shaped target volumes? Radiotherapy and Oncology 2009; 93:259-265.

55. Masi L, Doro R, Casamassima F. VMAT plan for treatment of prostate cancer: dosimetric verifications and comparison with IMRT. Poster session presented at: 10th Biennial ESTRO Conference on Physics and Radiation Technology for Clinical Radiotherapy: 2009 August 30- September 3; Maastricht, NH.

56. Fix MK, Keall PJ, Dawson K, Siebers JV. Monte Carlo source model for photon beam radiotherapy: photon source characteristics. Med. Phys 2004; 31:3106 – 3121.

57. Fippel M, Haryanto F, Dohm O, Nüsslin F. A virtual photon energy fluence model for Monte Carlo dose calculation. Med. Phys. 2003; 30(3):301-311.

58. Jelen U, Alber M. A finite size pencil beam algorithm for IMRT dose optimization: Density corrections. Phys. Med. Biol. 2007; 52:617–633.

59. Alber M. A concept for the optimization of radiotherapy [dissertation]. Germany: University of Tübingen; 2010. 59 p.

60. Semenenko VA, Reitz B, Day E, Qi XS, Miften M, Li XA. Evaluation of a commercial biologically based IMRT treatment planning system. Med. Phys. 2008; 35(12):5851–60.

61. Wu Q, Mohan R, Niemierko A, Schmidt-Ullrich R. Optimization of intensity-modulated radiotherapy plans based on the equivalent uniform dose. Int. J. Radiat. Oncol. Biol. Phys. 2002; 52:224–235.

62. Thieke C, Bortfeld T, Niemierko A, Nill S. From physical dose constraints to equivalent uniform dose constraints in inverse radiotherapy planning. Med. Phys. 2003; 30:2332–2339.

63. Lian J, Xing L. IMRT optimization including the biological parameter uncertainty. Medical Physics 2004; 9 (31).

64. Yang Y, Xing L. Clinical knowledge-based inverse treatment planning. Phys. Med. Biol.2004; 49:5101

65. Qi XS, Semenenko VA, Li XA. Improved critical structure sparing with biologically based IMRT optimization. Med. Phys. 2009; 36(5):1790-1799.

66. Levegrun S, Jackson A, Zelefsky M, Skwarchuk MW, Venkatraman ES, Schlegel W, Fuks Z,Leibel S, Ling C. Fitting tumor control probability models to biopsy outcome after three dimensional conformal radiation therapy of prostate cancer: pitfalls inducing radiobiologic parameters for tumors from clinical data. Int. J. Radiat. Oncol. Biol. Phys 2001; 51:1064–1080.

67. Lyman J. Complication probability as assessed from dose-volume histograms. Radiat. Res. 1985; Suppl. 8:S13–S19.

68. Meerleer GO, Vakaet LA, De Gersem WR, De Wagter C, De Naeyer B, De Neve W. Radiotherapy of prostate cancer with or without intensity modulated beams: a planning comparison,'' Int. J. Radiat. Oncol. Biol. Phys 2000; 47:639–648.

69. Fiorino C, Broggi S, Corletto D, Cattaneo GM, Calandrino R. Conformal irradiation of concave-shaped PTVs in the treatment of prostate cancer by simple 1D intensity-modulated beams. Radiother. Oncol. 2000; 55:49–58.

70. Wang X, Mohan R, Jackson A, Leibel SA, Fuks Z, Ling C. Optimization of intensity-modulated 3D conformal treatment plans based on biological indices. Radiother. Oncol. 1995; 37:140–152.

71. De Gersem W, Derycke S, De Wagter C, De Neve W. Optimization of beam weights in conformal radiotherapy planning of stage III non-small cell lung cancer: Effects on therapeutic ratio. Int. J. Radiat. Oncol. Biol., Phys. 2000;47:255–260.

72. Bortfeld T, Schlegel W, Dykstra C, Levegrün S, Preiser K. Physical vs. biological objectives for treatment plan optimization. Radiother. Oncol. 1996; 40:185.

73. Niemierko A. A generalized concept of equivalent uniform dose (EUD) (Abstract). Med Phys 1999; 26:1100.

74. Choi B, Deasy J. The generalized equivalent uniform dose function as a basis for intensity-modulated treatment planning. Phys. Med. Biol. 2002; 47:3579–3589.

75. Abramowitz M, Stegun IA. Handbook of mathematical functions with formulas, graphs, and mathematical tables. New York: Wiley-Interscience; 1984. 1046p.

76. Thieke C, Bortfeld T, Niemierko A, Nill S. From physical dose constraints to equivalent uniform dose constraints in inverse radiotherapy planning. Med. Phys. 2003; 30:2332–2339.

77. Stavrev D, Hristov B, Warkentin E, Sham N, Stavreva B, Fallone G. Inverse treatment planning by physically constrained minimization of a biological objective function. Med. Phys. 2003; 30:2948–2958.

78. Yang Y, Xing L. Clinical knowledge-based inverse treatment planning. Phys. Med. Biol. 2004; 49:5101–5117.

79. Thomas E, Chapet O, Kessler ML, Lawrence TS, Ten Haken RK. Benefit of using biologic parameters (EUD and NTCP) in IMRT optimization for treatment of intrahepatic tumors. Int. J. Radiat. Oncol. Biol. Phys. 2005; 62:571–578.

80. Alber M, Nüsslin F. An objective function for radiation treatment optimization based on local biological measures. Phys. Med. Biol. 1999; 44:479–493.

81. Monaco training guide. Report no LTGMON204.

82. Cho PS, Lee S, Marks RJ, Oh S, Sutlief SG, Phillips MH. Optimization of intensity modulated beams with volume constraints using two methods: cost function minimization and projections onto convex sets. Med. Phys.1998; 25: 435–443.

83. Nilsson G. Delta4 - A New IMRT QA Device. Med. Phys. 2007; 34: 2432.

84. James L Bedford J, Lee Y, Wai P, South C, Warrington A. Evaluation of the Delta4 phantom for IMRT and VMAT verification. Phys. Med. Biol. 2009; 54:167–176.

85. Geurts M, Gonzalez J, Serrano-Ojeda P. Longitudinal study using a diode phantom for helical tomotherapy IMRT QA. Caribbean Radiation Oncology Center.

86. Mayles P, Nahum A, Rosenwald J. Handbook of Radiotherapy Physics: Theory and Practice. 1st edition. UK: Taylor and Francis Group; 2007. ISBN- 978-0750308601.

87. Michalski JM, Gay H, Jackson A, Tucker SL, Deasy J. Rectal Radiation Dose-Volume Effects. Int. J. Radiation Oncology Biol. Phys. 2010; 76(3):S123–S129.

88. Viswanathan AN, Yorke ED, Marks LB, Eifel PJ, Shipley WU. Radiation dose–volume effects of the urinary bladder. Int. J. Radiation Oncology Biol. Phys. 2010; 76(3):S116–S122.

89. Craft D, Süss P, Bortfeld T. The tradeoff between treatment plan quality and required number of monitor units in intensity-modulated radiotherapy. Int. J. Radiation Oncology Biol. Phys. 2007; 67(5):1596–1605.

90. Thieke C, Küfer K, Monz M, Scherrer A, Alonso F, Oelfke U, Huber P, Debus J, Borfeld T. A new concept for interactive radiotherapy planning with multicriteria optimization: First clinical evaluation. Radiotherapy and Oncology 2007; 85:292–298.

91. Ottosson RO, Karlsson A, Behrens AF. Pareto front analysis of 6 and 15 MV dynamic IMRT for lung cancer using pencil beam, AAA and Monte Carlo. Physics in Medicine and Biology 2010; 55:4521-4533.

92. Van't Riet A, Mak AC, Moerland MA, et al. A conformation number to quantify the degree of conformality in brachytherapy and external beam irradiation: Application to the prostate. Int J Radiat Oncol Biol Phys 1997; 37:731–736.

93. Feuvret L, Noel G, Mazeron J, Bey P. Conformity Index: A review. Int J Radiat Oncol Biol Phys 2006; 64(2):333-342.

94. ICRU Report 83: Prescribing, recording, and reporting intensity-modulated photon-beam therapy (IMRT). Oxford, UK; 2010. 212 p.

95. Low D, Harms W, Mutic S, Purdy J. A technique for the quantitative evaluation of dose distributions. Med Phys 1998; 25:656-661.

96. Wetterstedt S. Dose Calculation Accuracy for a Flattening-Filter Free Photon Beam Implemented into Oncentra MasterPlan. [master thesis]. [Lund (Sweden)]: Lund University; 2007.45 p.

97. Wang L, Mok E, Xing L. Pros and cons of flattening filter free IMRT: A comparison with conventional IMRT with flattened beams. Med. Phys 2010; 37: 3375–3375.

98. Verbakel W, Cuijpers J, Hoffmans D, Bieker M, Slotman B, Senas S. Volumetric Intensity-modulated arc therapy vs conventional IMRT in head-and-neck cancer: a comparative planning and dosimetric study. Int. J. Radiation Oncology Biol. Phys. 2009; 74(1):252–259.

99. Palma D, Vollans E, James K, Nakano S, Moiseenko V, Shaffer R, McKenzie M, Morris J, Otto K. Volumetric modulated arc therapy for delivery of prostate radiotherapy: comparison with intensity-modulated radiotherapy and three-dimensional conformal radiotherapy. Int J Radiat Oncol Biol Phys. 2008; 72(4):996-1001.

100. Kopp RW, Duff M, Catalfamo F, Shah D, Rajecki M, Ahmad K.VMAT vs. 7-field-IMRT: assessing the dosimetric parameters of prostate cancer treatment with a 292-patient sample. Med Dosim. 2011; 36(4):365-72.